Global Production Networks and Asset Prices*

Teodor Dyakov† Hao Jiang‡

This Draft: March 2025

Abstract

We identify choke point industries in global production networks as strategic nodes bridging the flows across global value chains. We find that they tend to be in countries with deep seaports, better educated labor force, and more developed capital markets, and be industries relatively upstream in the value chains. Following China's accession to the WTO, many choke point industries migrated to China, shifting the topology of global production networks. Using the blockage of the Red Sea by the Houthis as a natural experiment, we find evidence of negative shocks propagating throughout global production networks via the important choke points—water transportation industries. In global stock markets, firms in the choke point industries earn higher stock returns than their peripheral peers by more than 6% per year, pointing to a link between globalized production and global asset pricing.

Keywords: Global Supply Chain, Choke Points, Production Networks, Asset Prices

JEL Classifications: F10, F30, G10, G12, G15

*We thank the participants in the seminar held at the National University of Singapore and University of Nebraska–Lincoln for helpful comments.

†EDHEC Business School. Address: 393 Promenade des Anglais BP 3116, 06202 Nice Cedex 3, France. Phone: +33 4 93 18 69 55. E-mail: teodor.dyakov@edhec.edu.

‡Broad College of Business, Michigan State University. Address: Eppley Center, 667 N. Shaw Lane Rm 332, East Lansing, MI 48824, USA. Phone: +1 517 3554109. Email: jiangh@broad.msu.edu.

1 Introduction

Since the 2020 global pandemic, disruptions to global supply chains have emerged as a sweeping force shaping economic fluctuations and market volatility. Emanating from such varied sources as pandemic-induced lockdowns, natural disasters, military conflicts, port congestions, and economic sanctions, the frequent disruptions exposed the fragility of the global production networks, which has received widespread attention from businesses, academics and policy makers (See, e.g., Lund et al., 2020; Baldwin and Freeman, 2022; Council of Economic Advisers, 2022; Grossman et al., 2023; The White House, 2021).

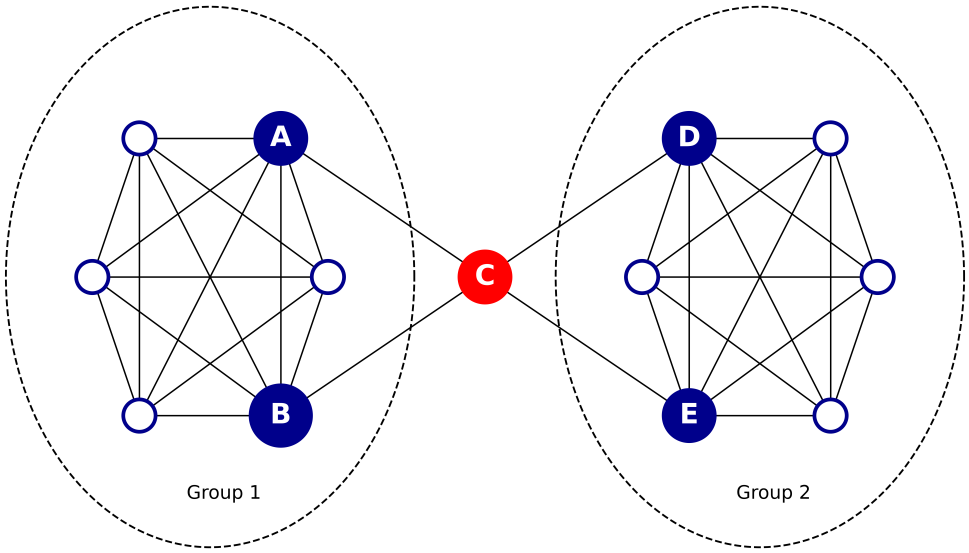
Inspired by a growing literature on the inherent fragility of production networks (See, e.g., Acemoglu and Tahbaz-Salehi, 2024; Elliott et al., 2022; Elliott and Jackson, 2024), we study the choke points in global production networks, which are structurally important for the network fragility, and explore their asset pricing implications in global stock markets. We use the term "choke point" to describe strategic locations in global production networks, analogous to how transporters use it to refer to important points in navigation paths such as the Bab el-Mandeb Strait connecting the Red Sea with the Gulf of Aden and Indian Ocean, and the Strait of Malacca connecting the Indian Ocean and Pacific Ocean, or similar to how military strategists flag important mountain passes crucial in a battle. In the networks space, choke points drive the flows across the nodes in the network, disruptions to which tend to break down the flows of the system. For global production networks, the choke points can drive the fragility of global production.

Our empirical strategy is to first build the global production networks based on a panel of world input-output tables compiled by the Organization for Economic Cooperation and Development (OECD). The resulting network covers 77 economies and 45 industries over the period from 1995 to 2020. It is directed and weighted based on the value-added in the world import and export data.

We identify the choke points in global production networks based on the geometry of production networks. In particular, we propose a novel measure of Choke Point Value (CPV) that captures strategic locations bridging the flows across global value chains. To build intuition for this measure, think of an economy's industry, node C, which interconnects two regional production blocs, Groups 1 and 2 in Figure 1. For simplicity, this network is undirected and unweighted. In this network, the two regional production blocs are well integrated within

each region. The global production network emerges by connecting the two regions through node C. As a result of this geometry, C plays a special role in bridging the flows of goods and services between the two production blocs. On the one hand, it expands the production opportunity set for both Group 1 and Group 2; on the other hand, the reliance of each group on the other through this choke point increases the fragility of global production. Disruptions to industry C, due to external shocks such as lockdowns or import/export restrictions, will have disproportionately large effects on the output of the global production. Intuitively, in this production network, nodes A, B, D and E are less important choke points, with the rest structurally the least important.[1]

Figure 1: Choke Points in a Hypothetical Global Production Network with Two Regionally Integrated Production Blocs



We compute the Choke Point Values for each economy-industry pair in our sample from 1995 to 2020. Our estimates depict global production networks with a slowly moving topology. In terms of choke point industries, the ranking tends to be relatively stable. Water Transportation, Wholesale and Retail Trade, Basic Metals, Information and Communication Technology (ICT) and Electronics, and Chemicals reshuffle their relative positions among the top five in-

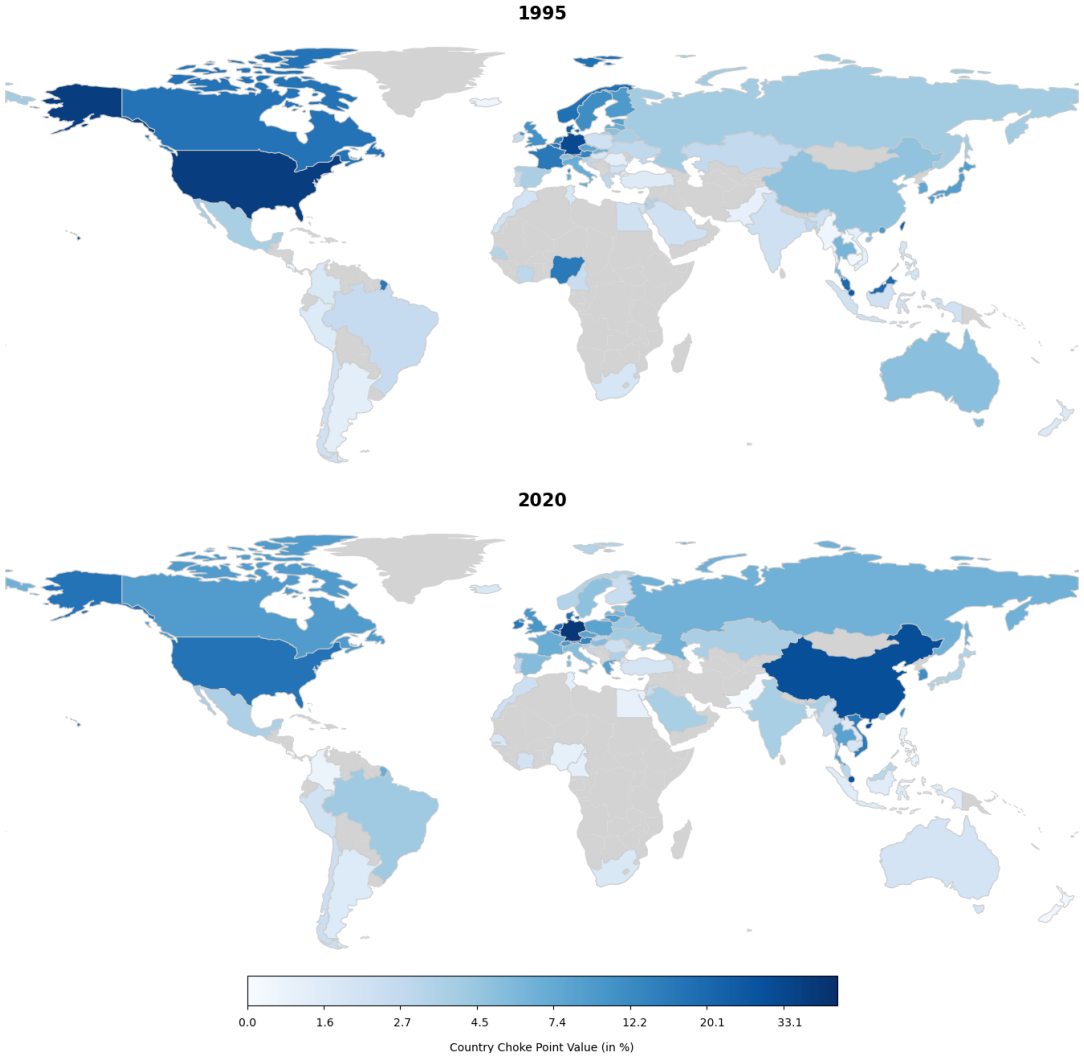
[1]Section 3 provides a formal definition of the Choke Point Value. It is notable here that popular degree-based centrality measures such as eigenvector centrality and page rank give the lowest score to node C in terms of centrality.

dustries with the highest CPVs in 1995 and 2020. An interesting change comes from the IT Services industry, which moves from the 35^{th} in 1995 to the 10^{th} in 2020. This change could reflect the increasing digitization of the global economy.

Larger shifts take place in the spatial distribution of the choke points, as illustrated in Figure 2. For instance, the United States in 1995 is the most important economy in terms of CPVs, which dwarfs Germany and Singapore. However, the US falls out of the top five countries, ranked as the 6^{th} in 2020. China leapfrogs in this period from the 35^{th} to the 2^{nd}, which is eclipsed only by Germany in 2020. Our analyses show that the secular decline of the US and the rise of China in global production networks in terms of choke point significance is expedited following China's entry into the World Trade Organization (WTO) in 2001.

Figure 2: Geographic Distribution of Choke Point Values Over Time

This figure depicts economy Choke Point Values for years 1995 and 2019, computed as the number of shortest paths passing via a economy, expressed as a percentage of all shortest paths. Higher intensity of blue represents higher economy Choke Point Value. Countries with no data are depicted in light gray.



At the economy-industry level, we find that a combination of economic, financial and geographic characteristics jointly determines the location of choke points in global production networks. In particular, choke points tend to come from economies endowed with deep seaports, with better educated labor force, and more developed capital markets. These findings are intuitive, because deep seaports are vital for low-cost and efficient transportation of an economy's imports and exports, and significant amounts of human capital and physical capital (backed by financial capital) are important for choke point industries to sustain their special positions in complex global value chains. Applying the upstreamness measure of Antràs et al. (2012), we also find that the choke point industries tend to be relatively more upstream. To gain intuition for this result, think of the Taiwan Semiconductor Manufacturing Company, which dominates the fabrication of logic chips. It is widely recognized as a critical choke point in the semiconductor industry, whose products constitute indispensable inputs to numerous sectors of the economy, including, e.g., energy, healthcare, agriculture, consumer electronics, manufacturing, defense and transportation (The White House, 2021).

After mapping out the choke points in global production networks, we study their asset pricing implications. There is a growing literature on how production networks propagate and amplify firm-level or sectoral shocks to the aggregate economy.[2] For instance, Acemoglu et al. (2012) provide a theoretical framework to show that idiosyncratic shocks to industries in an exogenous production network can lead to aggregate fluctuations through input-output linkages. Empirically, Carvalho et al. (2021) examine the impact of the 2011 Japanese earthquake and find that the resulting disruption propagates along supply chains, leading to a meaningful decline in the Japanese GDP.[3] More recently, this literature studies how endogenous production networks respond to exogenous shocks, and highlights the fragility in production networks, which has important macroeconomic consequences (See, e.g., Acemoglu and Tahbaz-Salehi, 2024; Elliott et al., 2022; Elliott and Jackson, 2024).

Building on this literature, we test two hypotheses. First, when choke points in global production networks are hit with negative shocks, industries with higher exposures to them are more negatively affected. Second, in global stock markets, choke point industries command a higher risk premium. The first hypothesis, in principle, can be tested using shocks to any

[2]For surveys of this literature, see, e.g., Carvalho and Tahbaz-Salehi (2019) and Baqaee and Rubbo (2023).

[3]Other examples include Acemoglu et al. (2016) and Barrot and Sauvagnat (2016).

industry. However, thanks to their special role in bridging global production networks, shocks to the choke points tend to have disproportionately larger effects along global value chains, which renders a more powerful empirical test. It also helps to lay an empirical foundation for the second hypothesis, which rests on the joint hypothesis that negative shocks to choke points have a nontrivial effect on aggregate productivity and that global productivity shocks are priced in the stock markets.

To test the first hypothesis, we use the Red Sea crisis as a natural experiment that disrupts water transportation industries. The Red Sea is a vital artery in maritime trade connecting Asia and Europe. From late 2023, the Houthis launched attacks on merchant and navy vessels passing through the Red Sea. On November 19, the Houthis hijacked a British-owned, Japanese-operated cargo ship. During the next two months, more than 30 vessels were assaulted in the region. In response to the dangers posed by the Houthi attacks, most shipping companies decided to take the much longer and more costly trade route around the Cape of Good Hope in Africa, to avoid the perils in the Bab el-Mandeb strait. For example, the largest water transport company in the world in terms of container capacity, A.P. Moller-Maersk announced on January 5, 2024 that all of its container ships will be diverted around the Cape of Good Hope for the foreseeable future. Since many affected water transportation industries have high choke point values in global production networks, we use this setting to test whether industries with higher exposures to choke point disruptions are hit harder.

To measure the exposure of an economy-industry pair to the Red Sea crisis, we count the number of shortest paths in the 2020 global production network that connect an industry in developed Europe with another one in (developed or developing) Asia Pacific. If the shortest path passes an interior node that is a water transportation industry (e.g., the Dannish water transportation industry), we label it as a treated shortest path. We compute the ratio of the number of treated shortest paths to the total number of shortest paths that originate from or end in an economy's industry as our measure of exposures for that industry to the Red Sea Crisis. The differences-in-differences estimates show that industries with higher exposures tend to perform worse after the Red Sea crisis, which supports the first hypothesis. For instance, we find that industries with a 10% increase in the exposures to the Red Crisis deliver a lower abnormal return of 1.68% per week during the first four weeks in 2024.

To test the second hypothesis, we construct industry stock portfolios for each node in the

global production networks. In each year from 1995 to 2020, we rank industries based on the Choke Point Value into five quintiles, with Q5 (Q1) representing the industries with the highest (lowest) CPV. We find that stocks in Q5 earn higher average returns than those in Q1 by more than 6% per year. This return spread cannot be explained by a battery of international asset pricing models. For instance, the annualized α on the spread portfolio long stocks in Q5 and short those in Q1 is 5.8% for the world CAPM and 7.2% for the international Fama-French 5-factor model augmented with the momentum factor.

Herskovic (2018) presents an asset pricing model with production networks, which features two systematic risk factors describing the state of the production network: network concentration and network sparsity. Applying his model to the US production networks, he finds that the sparsity factor has a positive price of risk and concentration factor has a negative price of risk. To examine the incremental effect of our choke point values, we estimate the sparsity beta and concentration beta for each industry portfolio in our sample. Then we perform double sorts on the CPV and sparsity beta and concentration beta, respectively. We find that stocks in the high CPV portfolios earn higher returns after controlling for the sparsity beta and concentration beta.

We also perform the Fama-MacBeth cross-sectional regressions, which control for a rich set of industry and economy characteristics. In our full specification controlling for the industry beta, log market capitalization, log book equity,[4] profitability, investment, dividends, past one-month return, past one-year return skipping the past month, log population of the economy, change in GDP per capita, inflation rate, currency return, local economy beta, concentration beta, sparsity beta, and transportation cost beta, the link between CPV and future stock returns remains economically strong and statistically significant.

Ahern (2013) studies network centrality and the cross-section of stock returns for the U.S. domestic production network. In particular, he constructs the network of inter-industry trade flows using the 1997 Input-Output tables from the U.S. Bureau of Economic Analysis. He finds that over the next five years from 1998 to 2002, industries with high eigenvector centrality earn higher average returns than those with low eigenvector centrality. To evaluate how our choke point estimates differ from other commonly used network centrality measures, we construct

[4]Following Koijen and Yogo (2019), we include log market capitalization and log book equity separately, instead of the log boo-to-market ratio. The results are intact when we use the log book-to-market ratio.

a battery of alternative measures including eigenvector centrality, Katz-Bonacich centrality, weighted indegree centrality, in-closeness centrality, weighted outdegree centrality, and out-closeness centrality. These alternative centrality measures have positive correlations with our CPV, but in the presence of CPV that is a strong predictor of stock returns, they do not have reliable return forecasting power in the Fama-MacBeth regressions. This result reinforces the importance of identifying choke points in the global production networks.

A growing literature studies how macroeconomic fragility can arise out of supply chain disruptions. For instance, Acemoglu and Tahbaz-Salehi (2024) present a theory of firms forming specific, productivity-enhancing customer-supplier relationships at costs. When a new link is formed between two firms, they do not fully internalize the resulting surplus, leading to inefficient production networks. Such inefficiencies result in equilibrium fragility in aggregate output: even small shocks can lead firms to drop one or more of their partners, which creates a discontinuous decline in aggregate output. Elliott et al. (2022) consider alternative sources of fragility in production networks. They analyze an economy in which firms produce complex goods with multiple essential inputs and many stages of production. They show that the equilibrium supply network can be fragile, with small shocks to the strength of supplier relationships generating precipitous contractions of aggregate production. Elliott and Jackson (2024) distinguish between short-term and long-run impact of supply chain disruptions in an international production network. They show that in the short term, the fragility of global supply chains increases with their complexity. Our main contribution to this literature is to empirically identify systemically important nodes in global production networks, i.e., their choke points, exploring their evolution, determinants and implications for risk premiums in the global stock markets. Our main message resonates with the theme in the literature: the fragility of global production networks is a source of risk crucial for the macroeconomy and global asset markets.

There is a nascent literature studying the link between evolving global supply chains and macro-finance. For instance, Antràs (2023) studies the relation between the secular decline in interest rates and the deepening of global value chains (the increase in the length of production chains); Kim and Shin (2023) examine the connection between the development of global supply chains and the dollar exchange rate. Our paper contributes to this literature by studying the link between global value chains and stock prices around the world.

Finally, our paper is related to the literature that studies the implications of production

networks for stock returns. For instance, Cohen and Frazzini (2008) and Menzly and Ozbas (2010) study stock return predictability through supplier-customer relationships. Ahern (2013) tests the relation between eigenvector centrality and industry stock returns. Herskovic (2018) proposes new risk factors based on the structure of production networks. Gofman et al. (2020) and Ramírez (2024) study the relation between firm-level production networks and their stock returns. However, these studies focus on domestic production networks; our main interest is in understanding the structural vulnerability in global production networks and how it influences asset prices. Moreover, our novel evidence on the propagation of the Red Sea crisis through global value chains contributes to the literature on the propagation and amplification of economic shocks through global production networks.

2 Sample Construction and Summary Statistics

We construct the global production network using yearly World Input-Output Tables (WIOTs) from the OECD spanning $J = 77$ economies (76 economies and an additional Rest of the World (ROW) economy) and $S = 45$ industries between 1995 and 2020. The WIOTs allow us to unpack the sources of value added embedded in the gross exports of each of the distinct 77×45 economy-industry pairs. The decomposition of the WIOT gross export data is referred to as Trade in Value Added (TiVA), and its final product is a $JS \times JS$ matrix decomposing gross exports in domestic and foreign value-added sources. We provide details on the methodology to unpack the sources of value-added in Appendix A.

In the resulting global production network, each node represents a distinct economy-industry pair for the 77 economies and 45 industries: $n(s, j)$ refers to industry s in economy j. The links or edges (denoted by e) in the network are directional and weighted, based on the TiVA. Specifically, edge $e_{i,j}^{r,s}$ is from node $n(r, i)$ to node $n(s, j)$ with weights based on the dollar value added of the gross exports of industry s in economy j that stem from the imported intermediate inputs from industry r in economy i, denoted as $VA_{i,j}^{r,s}$, which is scaled by the gross exports of industry s in economy j, GX_j^s.[5] Since we focus on global production networks, each edge where $i = j$ is by construction set to zero.

[5]The subscripts i and j index economies ($1 \leq i, j \leq 77$), and the superscripts r and s index industries ($1 \leq r, s \leq 45$). We use two subscripts and two superscripts to describe flows. The left subscript refers to the source (i.e., selling) economy and the right subscript refers to the destination economy. Similarly, the left superscript refers to the source industry and the right superscript refers to the destination industry.

We provide descriptive statistics of the global production network in Table 1. In total, there are 3465 nodes (77 $\times$ 45 economy-industry pairs). The value of the average edge is 0.006%. Consistent with the literature (e.g., Johnson and Noguera, 2017), we find that on average 21% of the value-added of each economy-industry stems from foreign sources (0.006 $\times$ 76 foreign economies $\times$ 45 industries). Because the network is directed and weighted, the reliance of a node on foreign sourcing (the sum of all edges ending in the node) can be very different than its importance as a supplier (the sum of all edges originating from the node). We show that the reliance on foreign sourcing is similar across geographical regions, but there are differences across regions in terms of their importance as suppliers. For instance, companies in the United States and Canada (region NAM) are relatively more important as suppliers of intermediary goods and services for foreign producers, indicating the importance of NAFTA for global trade. Across broader industry sectors, inputs from Mining and Quarrying represent the most value-adding foreign inputs in the global production network, while Manufacturing has the strongest reliance on foreign sourcing. Appendix B provides an overview of our sources of firm-level and economy-level data, used in the empirical tests.

3 Choke Points in the Global Production Network

We next identify choke points as strategic locations bridging flows across global value chains. To do this, we rely on the geometry of the constructed production network. Choke points act as intermediate nodes that lie on supply chain routes with heavy flows. Disruptions to such structurally important nodes are likely to impact many other nodes upstream and downstream and hence decrease the overall amount of flows in the production network. In contrast, disruptions to nodes that do not act as bridges in connecting other nodes are likely to have limited effect on the overall network. Our main measure measure of choke points relies on this intuition.

3.1 Shortest Paths Between Nodes

The global production network can be represented as a directed graph $\boldsymbol{G(V, E)}$ defined by the set of nodes $\boldsymbol{V}$ (i.e., the 77 $\times$ 45 economy-industry pairs) and the set of edges $\boldsymbol{E}$ (i.e., the directional flows between nodes). A *path* between two nodes $n(r, i)$ to $n(s, j)$ is an alternating sequences of nodes and edges, beginning with $n(r, i)$ and ending with $n(s, j)$, such that each

edge e connects its preceding with its succeeding node. In the example of the unweighted, undirectional network in Figure 1, the structurally important node C lies on all geodesic paths (i.e., the paths with the fewest possible edges) connecting nodes from Group 1 to Group 2. However, the global production network is weighted and directed. This means that the geodesic path between two nodes need not be the one with strongest flows. Among the many possible paths connecting $n(r,i)$ with $n(s,j)$, some are associated with large flows of goods and services (large values of e), while others not. Therefore, we determine the path from $n(r,i)$ to $n(s,j)$, with the strongest flows. This path represents a flow-weighted shortest path and and is usually referred to as *Minimum Cost Path* or *Weighted Shortest Path* (Opsahl et al., 2010). For simplicity, we label it as the *shortest path*.

The shortest path from node $n(r,i)$ to node $n(s,j)$ in the graph $\boldsymbol{G(V,E)}$ is given by:

$$ShortestPath_{n(r,i)\rightarrow n(s,j)} = \arg\min_{P} \sum_{e\in P} c(e) \tag{1}$$

where P represents a path in $\boldsymbol{G}$, and $c(e)$ is the cost of an edge e along the path P. As common in the network literature, we choose to assign a cost to each edge equal to e^{-1} (e.g., Brandes, 2001 and Newman, 2001). Thus, a low-cost edge is one with a strong connection between the two nodes. This path minimizes the total *cost* between industry r in economy i and industry s in economy j. To find the path with the lowest total cost, we apply the algorithm of Dijkstra (1959), similar to finding the quickest route in GPS navigation systems (Opsahl et al., 2010).

We illustrate this procedure with three shortest paths from the 2020 production network in Figure 3. In orange we track the direct and shortest paths that connect the Motor Vehicles industry in Sweden (the *source* economy-industry pair) with that in the USA (the *sink* economy-industry pair). The edge connecting the two nodes is small: less than 0.001% of the value added of the exports of the Motor Vehicles industry in the USA comes from imports from the Motor Vehicles industry in the Sweden. However, this direct (geodesic) path does not capture the economic importance of the flows between the two nodes. The shortest path connects the source node and sink node via the Motor Vehicles industries in Poland and Germany. All edges along this shortest path are relatively large and range from 0.29% to 0.54% and are at least 48 times larger than average edge size in the production network. Hence, the shortest path indicates a stronger importance of the Motor Vehicles industry in Sweden for the Motor Vehicles

industry in the USA than the direct (geodesic) path would suggest. Although this shortest path happens to be horizontal across the same industry across multiple countries, shortest path can also traverse vertically. For example, the shortest path in red connects Machinery in Turkey with Fabricated Metals in Japan, while the shortest path in blue connects the Rubber and Plastics industry in Israel with Machinery in Italy.

3.2 Computing Choke Point Values

We use the computed shortest paths to locate choke points in the global production network. The Choke Point Values are based on the intuition that choke points are more likely to occur for nodes that lie on relatively more of the computed shortest paths. In the example of Figure 3, the Motor Vehicles industry in Germany is likely to be a choke point as all example shortest paths pass through it. For each node we compute a Choke Point Value (CPV) as the total number of shortest paths passing via the node, scaled by the total number of shortest paths in the network. Specifically,

$$CPV_{v,t} = \sum_{j \neq k \neq v,t} \frac{\sigma_{jk,t}(v)}{\delta_t}, \tag{2}$$

in which v is a production node (an economy's industry) in the global value chain, j and k are two distinct production nodes other than v, t is the calendar year, $\sigma_{jk,t}(v)$ is the number of the shortest paths from j to k passing through v, and δ_t is the total number of shortest paths in the network ($\sum_{j \neq k,t} \sigma_{jk,t}$). CPV is conceptually similar to the class of centrality measures referred to as *betwenness centrality* (see Freeman, 1977) and most closely resembles the flow-based betweenness centrality introduced by Freeman et al. (1991). As common in the network literature, we cross-sectionally standardize our flow-based betweenness centrality to lie between zero and one. For some exercises, we compute economy or industry-level Choke Point Values. These measures are constructed analogously to the baseline economy-industry level CPV, where we consider either countries or industries as nodes. For example, when we compute the CPV for the USA, we compute the fraction of all shortest paths passing via the economy. To aid with understanding of the economic magnitude of the CPV, we sometimes express CPV as unstandardized flow-based betweenness in percentages.

Our CPV measure implicitly assumes that flows across the supply chain cannot easily

be re-allocated via different paths. Flows in the production network do not diffuse randomly across different paths, but rather follow a pre-determined path from a source to a sink node, based on economic fundamentals. Thus, the shortest paths and betweenness centrality may not be suitable for studies of the spread of infections or beliefs. However, they are suitable for studying the flows of goods and services where we can identify economically important links between nodes that cannot easily be replaced (Borgatti, 2005). For example, the shortest path depicted in red in Figure 3 captures how a metal part manufactured in Turkery is used to produce a component of a gearbox in Hungary which then is used by a German company in the Motor Vehicles industry to deliver an advanced gearbox for a mining machine in South Africa that mines metals for the Fabricated Metals industry in Japan. The high-value added activities in the German Motor Vehicles industries cannot easily be offshored to another economy. The higher the number of such economically important routes that pass through the German Motor vehicles industry, the higher its importance as a choke point in the global production network. There are many other paths connecting the Turkish Machinery industry with the Fabricated Metals industry in Japan. However, by construction they cover a smaller flow and we thus implicitly assume they are easier to replace and hence less important for the overall connectivity of the network. This example also illustrates a potential disadvantage of betweenness centrality as there may exist paths with relatively lower flows that could be harder to substitute than the flows along the more intensive shortest path.

3.3 Mapping the Choke Points in the Global Production Network

We provide descriptive statistics of the Choke Point values in Panel A of Table 2. The average CPV is 0.007 and 40% of all economy-industry pairs have a CPV of zero. The most important economy-industry pairs stem from developed countries and East Asia (e.g., China) and are part of the Manufacturing and Business Services sectors. In Panel B, we provide descriptive statistics for a subsample of economy-industry pairs for which we have sufficient financial data to construct our stock portfolios. In total, this subsample spans 358 economy-industry pairs from 41 economies, most of which are from the Manufacturing and Business Services sectors. In general, the economy-industry pairs part of our stock sample come from economies and

industries with relatively high CPV.

We visualize the countries with highest CPV in Figure 4, separately for 1995 and 2020. The size of each node indicates the economy's CPV (expressed in percentages) and the thickness of the lines between any two countries indicate the number of shortest paths going between them. Thus, the thicker the line, the more important the connection between two countries is for determining choke points. Because the shortest paths are directed, the number of shortest paths passing from economy A to economy B can be very different from the number of shortest paths passing in the opposite direction. We group nodes geographically and in terms of economic development following the classification in Table 1. We place the eight countries with highest CPV inside each graph, and and all other countries in a circle on the outer side.

There are significant changes in the distribution of economy-level CPV between 1995 and 2020. Most notably, the USA is the economy with the highest CPV in 1995, but its importance as a choke point has decreased by 2020 when it ranks only 6^{th}. China, while largely unimportant in terms of CPV at the start of the sample, is the second highest ranked economy in 2020. Germany is ranked 2^{nd} at the start of the sample but has steadily become even more important in the global production network, ranking 1st at the end of our sample. By the end of our sample, 40% of all of the computed shortest paths pass through at least one industry from Germany, primarily from the manufacturing sector. We also observe a shift in the importance of supply chain flows moving away from North America to Asia, as evidenced in the changes of the number of shortest paths passing via the countries in the graph (the thickness of the lines).

We visualize changes in the ranking among the the top 10 countries and industries between 1995 and 2020 in Figure 5. In Panel A, we track the development of CPV for the top 10 countries. The importance of Singapore is mainly due to the economy's central role in moving commodities and other products across the world, while that of Taiwan is because of the economy's central role in the ICT and Electronics industry. The importance of Water Transportation is exemplified with the central role of shipping and warehousing services from Denmark and Norway. We also note the increase in CPV for Ireland, moving from the 48^{th} place in 1995 to 7^{th} in 2020, largely due to its increased importance as an offshore hub. In Panel B, we plot CPV for the top ten industries. Not surprisingly, the movement of goods is at the center of the global production network, with Wholesale and Retail and Water Transport being the two most central industries. The most important manufacturing industries are ICT and

Electronics, Basic Metals, and Chemicals. Thus, choke points are likely to map to industries that provide essential inputs to foreign manufacturers.

We next visualize the most granular version of choke points using the global production network in 2020 (Figure 6). Each node in the graph represents an economy-industry pair. The size of each node indicates the node's CPV and the thickness of the lines between nodes $n(r,i)$ and $n(s,j)$ indicate the number of shortest paths going via $n(r,i)$ and then $n(s,j)$. We group the economy-industry pairs geographically and in terms of economic development following the classification in Table 1. In addition, economy-industry pairs within each region are grouped in three concentric circles, with the outer one covering manufacturing, the middle one business services, and the inner one covering all other sectors.

The Wholesale and Retail industry in Singapore has the highest CPV in the 2020 global production network. That industry contains Olam International Ltd which is a leading food and agribusiness firm that sources and processes food, ingredients, feed and fibre around the world, with value chains spanning more than 60 countries. In second and fourth place are the Chinese and Taiwanese ICT and Electronics industries, highlighting the global importance of companies such as the Taiwan Semiconductor Manufacturing Company (TSMC) – the first pure-play semiconductor foundry in the world, which dominates the contract foundry market. The shortest paths passing via those industries are among the most numerous, highlighting the importance of potential disruptions to these industries for the global economy. Denmark Water Transport is another economy-industry pair with high CPV, highlighting the importance of A.P. Moller-Maersk as the main container shipping company in terms of container capacity during our sample. German companies are central for the flow of goods and services in the manufacturing sector, with the Chemicals, Motor Vehicles, and Basic Metals among the main choke points.

4 Determinants of Choke Points

We next study the county-level determinants of choke points in the global production network in a panel regression of CPV on lagged economy characteristics and upstreamness:

$$log(CPV)_{s,j,t} = \mu_t + \beta \times \mathbf{Z}_{j,t-1} + \gamma \times upstreamness_{s,j,t-1} + \epsilon_{s,j,t} \tag{3}$$

The dependent variable in our panel regressions is log of one plus unstandardized CPV, computed for each pair of economy s and industry j at the end of year t. We use the unstandardized version of CPV since it reflects potential time-series changes in the intensity of flows within the production network. We include a set of lagged economy characteristics in $\mathbf{Z}$, lagged upstreamness (specific to each economy-industry pair), and year fixed effects μ_t.

Results are reported in Table 3. We first consider a measure of economy development $GOVERNANCE$, computed as the average of the World Governance Indicators of the World Bank across six dimensions, including voice and accountability, political stability, government effectiveness, regulatory quality, rule of law, and control of corruption. We find that choke points tend to be located among countries with higher quality of $GOVERNANCE$ (specification (1)), signifying the importance of the quality of institutions for the geographical location of vital industries in the global economy. In specification (2) we include $log(EDUCATION)$ that captures the availability of educated forces, measured as the log of the percentage of the population with tertiary education. In specification (3), we consider a measure of the development of capital markets $log(MCAP\ TO\ GDP)$, computed as the log of the market captialization of publicly traded companies relative to GDP. Both variables are statistically significant determinants of where choke points are located. The results indicate that choke points are likely to occur among industries with skilled labour force and high value added backed by the availability of financial capital, whose goods and services are essential components for the rest of the economy. For example, some of the highest CPV economy-industry pairs include the ICT and Electronics industry in Taiwan and the Motor Vehicles industry in Germany, both of which rely heavily on an educated workforce and reliable long-term financing. In specification (4), we include an index of the the three variables $AVE\ DEVELOPMENT$, computed as the average across the governance, education, and capital market developments variables.

We further show that choke points develop due to geographical endowments, allowing them to become a backbone for global trade. Specifically, we compute $DEEP\ PORTS$ as the number of deep-water ports within the economy. A deep-water port allows large marine freight vessels to dock and load and unload cargo and is thus likely to develop import and export capacities and increase the global integration of domestic industries. The significant coefficient on $DEEP\ PORTS$ in specification (5) supports this argument. In specification (6) we include further measures of size and economic development. Among those variables, only interest rates

have a statistically impact on CPV (alebit it only on the 10% level only), indicating that choke points tend to locate in economically more stable countries.

Last, in specification (7) we include economy-industry upstreamness (Antràs et al., 2012). The variable captures how many production stages the outputs of a given economy-industry pair are away from final demand. The more stages (i.e. intermediate downstream production nodes) it takes to reach final demand, the higher the upstreamness. We find that upstreamness is a strong predictor of where choke points locate. Industries, such as Water Transport and Wholesale and Retail are essential for the movement of raw goods before they are used as inputs in manufacturing. This stage of the supply chain is relatively upstream. As another example, consider the Taiwan Semiconductor Manufacturing Company. A recent report by The White House (2021) outlines, the company is a critical choke point in the global semi-conductor supply chain. It is also located relatively upstream and it provides inputs to numerous sectors located relatively downstream.

Removing barriers to trade can increase a economy's involvement in the global production network. The most significant event related to tariffs and trade liberalization in our sample is China's accession to the World Trade Organization (WTO) in 2001. As part of its WTO commitments, China reduced tariffs on a wide range of goods, essentially making Chinese markets more accessible to foreign goods and services. In return, other WTO members also made commitments to lower their tariffs on Chinese goods following the WTO's principle of Most-Favored-Nation (MFN) treatment. Although China's liberalization had already started in the 1980s, its accession to WTO leads to an increased integration in the global production by enhanced exports, foreign direct investment, and productivity (e.g. Brandt et al., 2017, Erten and Leight, 2021).

We show that China's accession to WTO had a large impact on the positions of choke points in the global production network. We use a economy-level measure of choke points as the total number of all shortest paths passing via the economy's domestic industries. We regress this economy level CPV on indicator variables for China, the post-2001 period, and their interaction. Results are reported in Table 4. In specification (1), we find a significantly positive coefficient on the interaction. Thus, China's accession to the WTO is associated with an increased importance of Chinese firms as intermediate nodes in the global production network. At the same time, the importance of industries in the USA has decreased. We show this by

conducting the same analysis for the USA: the economy dummy interaction with the post-2001 period has a significantly negative coefficient (specification (2)). We include the two effects in specification (3) and further control for economy-level determinants in specification (4) and find consistent results. The effect of China's accession to the WTO is economically large – following the WTO accession, 13.5% of all of the shortest paths in the world have moved to China (estimated coefficient of 0.751 in specification (4) times 18 years in the post-2001 period).

We visualize the impact of China's accession to WTO in Figure 7. The size of China's bubble represents the fraction of all shortest paths in the world that pass through the economy. In 1999, for example, 9.3% of all of the shortest paths passed via China. We group the rest of the countries together in groups, with the arrow going from the region towards China representing the total fraction of the shortest paths originating from the region that pass through China. For example, in 1999, 4.2% of the shortest paths originating from USA and CAN flowed via China (region North America). After the paths pass through China, they would eventually sink into the same or another region, driving the size of that region's bubble. For example, in 1999, the shortest paths ending in USA and CAN that have passed via China constituted 8.1% of all of the shortest paths ending in the region. This graphical representation allows us to visualizle the organization of the production network around China's accession to WTO.

Within two years of China's accession to WTO, the CPV of China increased to 21.6%. That is, 21.6% of all of the world's shortest paths flow via the economy by 2004, signifying the drastic increase in the importance of China in the global production network. We observe the largest increase in trading paths originating in Asia-Pacific (both Developed and Emerging, colors blue and green) that pass through China and end in USA. We also observe that 35.6% of all of the shortest paths ending in USA and Canada pass through China within two years of the accession. Thus, the graph illustrates the large shifts in global production following China's accession to the WTO with a) an increased importance of Chinese industries as bridge nodes, and b) the increased dependence of global customers on processed goods from China, particularly in USA and Canada.

We visualize the impact on USA in Figure 8. Following China's accession to the WTO, nearly half of all of the shortest paths passing via USA relocate elsewhere in the global production network. For example, we observe that 36.3% of all of the shortest paths originating from Developed Europe in 1996 were passing via the USA. By 2004, the number decreased to 19.7%.

The links from Asia-Pacific also experience substantial decreases, while naturally the links with Canada and Latin America (e.g. Mexico) were not affected by the WTO accession of China. In sum, China's accession to WTO was a major event that lead to the relocation of choke points away from USA to China.

5 Choke Points and Asset Prices

The choke points in global production networks have a number of distinguishing characteristics. First and foremost, they sit on strategic positions in global production networks, where many shortest paths connecting different nodes in the network pass through. As a result, disruptions to the choke points can influence a wide range of different industries across various economies, leading to cascading effects in a complex economic system. The amplification mechanism of choke point disruptions is similar to how failures at critical nodes in the power grid lead to major power outages such as the 2003 Northeast Blackout (See, e.g., Kinney et al., 2005 and Barabási and Pósfai, 2016). Second, the choke points tend to have low sustainability, thanks to, e.g., their superior geographic locations, knowledge and knowhow in producing particular components or products, and other comparative advantages. As a result, at least in the short run, the disruptions to the choke points in global production networks can lead to costly consequences.

Combining these observations with the insights from the literature on how firm- or sector-level disturbances propagate into non-diversifiable aggregate shocks as reviewed in the introduction, we derive two testable hypotheses using stock market data. First, when choke points in global production networks are hit with negative shocks, stock prices in the industries with higher exposures to them, i.e., with more shortest paths passing through them, are more negatively affected. Second, in global stock markets, choke point industries command a higher risk premium.

5.1 Propagation of Shocks from Choke Points to Connected Nodes

To test the first hypothesis, we use the recent attacks by Houthi militants on vessels passing through the Red Sea through the Bab el-Mandeb Strait and the ensuing crisis in water transportation as a natural experiment. The Red Sea is a vital artery in maritime trade connecting

Asia and Europe. Prior to the Houthi attacks, there would typically be more than 100 container ships passing through the Bab el-Mandeb strait connecting the Red Sea-Suez Canal and the Gulf of Aden (Figure 9). According to the World Economic Forum, this trade lane accommodates approximately 30% of the world's container traffic with a total annual movement of more than $1 trillion in goods. Since the second half of 2023, the Houthi militants in Yemen have been using sophisticated weaponry to target the container ships passing through the Bab el-Mandeb strait. On November 19, the Houthis hijacked a British-owned, Japanese-operated cargo ship. During the next two months, more than 30 vessels were assaulted in the region. In response to the dangers posed by the Houthi attacks, most shipping companies have decided to take the much longer trade route around the Cape of Good Hope in Africa and thus avoid the tensions in the Bab el-Mandeb strait. For example, the largest water transport company in the world in terms of container capacity A.P. Moller-Maersk announced on January 5, 2024 that all of its container ships will be diverted around the Cape of Good Hope for the foreseeable future.[6] A typical container ship going from Singapore to Rotterdam would normally take 26 days via the Red Sea (8,500 nautical miles), but after the rerouting via the Cape of Good Hope it would take 36 days (11,800 nautical miles). Starting from December, the number of container ships passing through the Bab el-Mandeb strait declined by more than 50% (Figure 9). Moreover, the freight rates on container ships carrying goods from Asia to Europe and vice versa had been steadily increasing from $960 for container at the end of October 2023 to $4,800 per container by mid January (Figure 10). The Houthi attacks created a substantial disturbance to a key choke point in maritime trade and global production networks, offering an ideal setup to test how idiosyncratic shocks propagate from a key choke point throughout global production networks.

We first identify the shortest paths affected by the disruption. We consider a shortest path to be affected if it meets all of the following requirements: (1) it originates from an industry in Developed Europe and ends in one in Developed or Emerging Asia Pacific, or in the opposite direction; (2) it includes a Water Transport industry as an interim node; and (3) it does not pass any industry in an economy located in North or South America. The first two criteria ensure that the resulting shortest paths contain a maritime trade route connecting economies in Western Europe and those in the Asia Pacific. The third criterion excludes the Trans-Pacific route and Asia-North America route via the Panama canal as the primary shipping route. The

[6]See `https://www.reuters.com/world/middle-east/maersk-diverts-vessels-away-red-sea-for-foreseeable-future-2024-01-05/`

remaining most natural shipping route in the shortest path connecting developed Europe and Asia Pacific passes through the Bab el-Mandeb strait. We apply these criteria to identify the treated shortest paths based on the 2020 global production network.

In Table 5, we provide descriptive statistics of the top five Water Transport industries affected by the Houthi attacks. The highest CPV-ranked Water Transport industry is from Denmark: the 3$^{\text{rd}}$ among all the economy-industry pairs in the 2020 global production network. Its CPV is based on 1,800,144 shortest paths that use it as an intermediary node. From those, we identify 21,5781 (12%) as affected by the Houthi attacks. The percentage affected shortest paths is even higher among the other most affected Water Transport industries. The results in this table indicate that the Houthi attacks resulted in a large economic shock to some of the most central economy-industry pairs in the global production network.

In Figure 11 we visualize the propagation of the shock across the world. The thickness of the solid arrows from the Bab el-Mandeb strait to any other economy represent the number of shortest paths connecting the strait with that economy. Thus, the more solid the line, the stronger the propagation of the shock. The three most important propagation routes are all vital trade links within Asia: the Bab el-Mandeb strait to Singapore, Singapore to Taiwan, and Taiwan to China. For each economy, we sum the total number of affected shortest paths originating or ending in it, and express it as a percentage of all shortest paths originating or ending in the economy. The higher the percentage of shortest paths affected by the Houthi attacks, the higher the intensity of blue. In Asia, Singapore plays a crucial role for the propagation of the shock. Although it has a relatively strong direct connection to the origin of the shock, the economy acts as an intermediate node connecting flows from and to other Asian countries. We also note that the top 3 most affected countries in Europe are Finland, Sweden and Norway. Their exports are heavily integrated into global trade networks, passing via major transport hubs such as Rotterdam, Hamburg, and Antwerp before reaching their final destination in Asia. Sweden and Finland are also heavily reliant on raw materials, chemicals and electronics that pass through European intermediaries before reaching them.

To measure the shock's impact on the Water Transport sector, we investigate the abnormal returns on firms in the top five Water Transport industries, most affected by the Houthi's attacks. For each stock, we estimate a CAPM model during the 52 weeks prior to the end of September 2023, where the market factor is computed as the value-weighted returns on all the

stocks in our global sample. We choose to end the estimation mode at the end of September as the Houthi began attacking targets in October. We use the estimated betas to compute weekly alphas as realized excess returns minus the product of the estimated betas and the realized excess return of the market. We plot the the cumulative value-weighted alphas of all selected Water Transport stocks in Figure 12. As tensions increased in November and December 2023, affected Water Transport companies experienced negative alphas, although most of the effect was reversed by the end of the year. However, as container prices spiked in early January (Figure 10) and maritime trade moved decisively away from the Bab el-Mandab strait, (Figure 9) the prices of affected companies plummeted. By then of March 2024, the cumulative alpha decreased by more than 30%. Thus, the Hotuhi's attacks resulted in a substantial shock to the performance of Water Transport industries operating in the Red Sea.

We next provide a direct test of our prediction that industries with stronger exposures to the Red Sea crisis are more negatively influenced. For each affected shortest path, we observe the source and sink node. Next, for each economy-industry pair, we sum the total number of affected shortest paths originating or ending in it, which is divided by all the shortest paths originating or ending in the node. The resulting percentage ratio, i.e., the fraction of all the shortest paths that are treated, is labeled as *Exposure*. It measures how strongly an economy-industry pair is influenced by the Red Sea crisis. By construction, we assign a score of zero to all the economy-industry pairs in North and South America.

We run a standard difference-in-differences regression to identify the magnitude of impact. The regression is specified as follows:

$$\hat{R}_{s,j,t} = \alpha + \theta \times log(Exposure_{s,j}) + \lambda \times log(Exposure_{s,j}) \times Post + \delta \times \mathbf{X}_{s,j} + Economy_s \times Sector + Week_t + \epsilon_{s,j,t}, \tag{4}$$

where the dependent variable is the abnormal return on the portfolio of stocks in the economy s, industry j pair in week t, computed in the same way as the weekly alpha on individual stocks used in Figure 12. We compare the effect of *Exposure* before and after the spike in container prices by interacting the variable with an indicator variable *Post*, which equals one for any week in 2024 and zero otherwise. $\mathbf{X}_{s,j}$ is a vector of control variables, computed at the end of November 2023. Because the largest price increase on freight rates occurred on the first day of January (220% relative to the last day of December, see Figure 10), we use January 1

2024 as the event day in our difference-in-differences regressions. Each specification includes week-fixed effects $Week_t$. In some specifications, we also include Economy×Sector-fixed effects. The isolate the effect of the shock, the sample periods includes the 4 weeks prior to the end of 2023 and the first 4 weeks in 2024.

We report the results in Table 6. In specification (1), we include the log of $Exsporue$ together with week fixed effects. The coefficient is statistically insignificant, indicating a lack of trends prior to the treatment. However, in specification (2), the interaction of log $Exposure$ with the indicator variable is significantly negative. It shows that economy-industry pairs with strong dependence on supply chains via the Red Sea experienced a decrease in stock prices during the treatment period. In tersm of magnitudes, a 10% increase in the fraction of treated paths results in a 1.68% decrease in weekly abnormal returns during each of the first four weeks of 2024. This is an economically large affect. When we include additional controls and economy×sector fixed effects in specifications (3) and (4), we find that the results are robust.

The design of our $Exposure$ variable reflects the idea that negative shocks can propagate through the shortest paths in global production networks. The resulting impact can be viewed as 'global' effects arising from the Red Sea crisis. As a placebo test, we also construct a measure based on direct links of an economy-industry pair with the water transport industries. For each industry in Developed Europe and Asia Pacific, we compute the weighted sum of direct links between the industry and water transport industries, with the weight equal to the edge of a link. This $DirectLink$ measure captures the 'local' effects of the Red Sea crisis. We expect the local effects to be weaker than the global effects. Column (5) examines this conjecture: we run a regression similar to Column (4), replacing the $Exosure$ variable with the $DirectLink$ variable. We find that the interaction of log of $DirectLink$ with $Post$ is negative, but statistically indistinguishable from zero. Overall, the results in Table 6 show that the negative shock to Water Transport industries due to the blockage of the Bab el-Mandeb strait cascaded through the global supply chains, which highlights the importance of choke points in bridging flows along multiple stages of global production.

5.2 Choke Points and Returns: Portfolio Sorts

Our second prediction stipulates that choke points have higher expected returns than their peripheral counterparts. To test this prediction, we construct value-weighted portfolios of pub-

licly traded stocks within each economy-industry pair, and study their returns in relation to CPV. At the end of each quarter, we sort economy-industry pairs into quintile portfolios, based on their CPV. We next track their returns during the next year, after which we rebalance. Note that we value-weight stocks within each economy-industry as well as within each portfolio. Hence, the total portfolios are also value-weighted. In Panels A and B of Table 7, we present the portfolios' excess returns and risk-adjusted returns, using an asset pricing model consisting the global Fama-French 5 factors plus Momentum.

We find that the returns of top CPV portfolio (Q5) exceed those of the bottom CPI portfolio (Q1) by more than 6% per year. The risk-adjusted performance shows similar magnitudes. and we find a monotonically-increasing pattern of risk-adjusted returns. The top portfolio delivers an alpha of 0.21% per month ($t = 2.51$), while the bottom portfolio acts as a hedge with an alpha of -0.40% per month ($t = -2.97$). The spread of 0.60% per month is highly statistically significant ($t = 3.87$). Thus, choke points command both a statistically significant and an economically large premium. We further find a pattern of increasing market beta with CPV. This finding is in line with our prediction that choke points contribute more to aggregate fluctuations.

In Panel C, we examine the robustness of our findings and report alphas for the spread portfolio using alternative risk-adjustment models. Following Bekaert et al. (2009), we compute alphas from two global CAPM models taking into account time-varying exposures to a global and a local portfolio. During our sample period, emerging economies have largely increased their share in global trade, pointing to potential time-variation in their exposures to global risk. To take this into account, each month we compute betas using the previous 36 months of economy-industry returns and a value-weighted index of all non micro-cap stocks in Compustat. Next, we use the estimated loadings and this month's realization of the world market portfolio to compute alphas. We again value-weight all alphas, after which we re-estimate betas and proceed with next month's alphas. The result from this World CAPM ($WCAPM$) model show a similar spread in performance between the top and bottom portfolios. We augment the model using a value-weighted local portfolio, covering all stocks within the region of the economy-industry pair. We follow the same classification used to allocate countries to regions based on geographical location and economy development as in Table 1. Following Bekaert et al. (2009), we orthogonalize the local factor to the global market portfolio and estimate time-varying

exposures as in the $WCAPM$ model. The alphas from this World-Local CAPM ($WLCAPM$) are economically smaller, but still statistically different from zero. For further robustness, we also present alphas for the spread protfolio using different subsets of the six factor model used in Panel A and find consistent results. Finally, we also compute using local Fama-French models, where we assign each economy-industry pair to its closest set of local Fama-French factors, available on Ken French's website. Similarly to the $WCAPM$ and $WLCAPM$ modes, each month we estaimte varying betas using the previous 36 months and then use the estimated betas and this month's factor realizations to estimate this month's economy-industry alpha. We value-weight alphas within each portfolio and the compute average alphas per portfolio. Again, we find that the spread portfolio exhibits positive alphas that are statistically different from zero.

5.3 Double Sorts

Herskovic (2018) studies changes in the topology of the production network over time and finds there are two network characteristics with asset pricing implications: network sparsity and network concentration. Sparsity quantifies the distribution of the size of the edges, while concentration characterizes the distribution of the sizes of the nodes. He shows that innovations in concentration and sparsity factors are priced risk factors. The main differences with us is that his focus is on the time-variation in the network topology within the USA while ours is on the cross-sectional differences in choke points around the world.

Differences in the location of choke points may reflect changes in the network sparsity and concentration. To investigate this possibility, we track the returns of industry portfolios double sorted on network concentration betas (or network sparsity betas) and CPV. We report alphas in Table 8. We find that CPV has an explanatory power over and above the economy-industry pairs' betas with network concentration (Panel A) and network sparsity (Panel B). Thus, the abnormal returns associated with choke points cannot be attributed to the changes in the network topology studied by Herskovic (2018).

In addition, economy-industry pairs that act as choke points in the global production network are likely to be larger in size. To disentangle the impact of size and choke points, we double sort economy-industry pairs in portfolios based on market size and then CPV. The abnormal returns of the portfolios are presented in Panel C of Table 8. We find that economy-

industry pairs with a large market capitalization have high abnormal returns only when they also have high CPV. When the CPV of large economy-industry pairs is low, their abnormal returns are negative. The spread between high and low CPV economy-industry pairs is statistically different from zero. Thus, the information content of choke points is not captured in their market capitalization.

5.4 Choke Points and Returns: Fama-MacBeth Regressions

To examine the robustness of our findings, we perform Fama-MacBeth regressions of monthly economy-industry pair excess returns on lagged CPV, controlling for industry and economy characteristics. Results are reported in Table 9. To ease the interpretation of the estimated coefficients, we use the percentile of betwenness, ranging from 0 to 100. In specification (1), we include the economy-industry beta, book equity, and market equity.[7] The estimated coefficient of the CPV percentile is 0.004 ($t = 2.79$). This is an economically large effect. For instance, going from the 50^{th} to the 60^{th} percentile translates into $10 \times 0.004\% \times 12 = 0.5\%$ per year. In specifications (2) and (3), we include several other characteristics, known to predict returns. In specification (4) we additionally include economy-level variables. The results are consistent. Last, in specification (5) we include a economy beta and betas with respect to network concentration and network sparsity (Herskovic, 2018). Because Barrot et al. (2019) show that firms in low shipping cost industries have a higher risk of displacement and carry a risk premium, we further include a beta with respect to transportation costs. Again, the effect of CPV on subsequent stock returns remains statistically significant. Overall, the excess returns associated with choke points cannot be attributed to industry and economy-level characteristics.

5.5 Alternative Measures of Centrality

Our Choke Point Value is based on betwenness centrality which counts the number of shortest paths passing via a node. According to this measure, choke points are likely to occur among nodes of the production network with heaviest transits of flows. In addition, choke points may occur in nodes with heavy flows that either end or originate from the node. We therefore construct measures of foreign dependence and foreign influence and study their relationship to

[7] We estimated an economy-industry beta using a CAPM model and 60 months of past monthly data. We require at least 24 available monthly returns to compute the betas. We estimate economy betas and betas with respect to transportation costs in a similar way.

CPV and future returns. Appendix C provides a definition of all centrality measures with a correlation matrix in Table A1.

There are several measures of foreign dependence, used in the literature. The impact of first-degree connections is captured by *weighted indegree*, which sums all edges leading to a node. In our setup, that translates to the total reliance on foreign sourcing of an economy-industry pair. Since a node influences a node that influences another node, we can compute the sequential impact *eigenvector centrality*. Nodes with high eigenvector centrality are strongly dependent on inputs from other nodes, which in turn are strongly dependent on others, etc. Closely related to eigenvector centrality is *Katz-Bonacich centrality*, which has an additional parameter that can adjust the influence of distant nodes (Katz, 1953; Bonacich, 1987). Economy-industry pairs with highest values on these centrality measures typically come from the manufacturing sectors of countries who are resource-dependent on foreign countries.

The weighted indegree, eigenvector centrality and Katz-Bonacich centrality essentially capture the same information, with correlations among them higher than 0.96. Ahern (2013) uses eigenvector centrality to show that central industries in the USA domestic network command a risk premium. We assess the information content of CPV relative to eigenvector centrality by including both measures in predictive Fama-MacBeth regressions. The results, reported in specification (1) of Table 10, show that CPV explains future returns over and above the eigenvector centrality. Using Katz-Bonacich and weighted indegree, we find similar results (specifications (2) and (3). In addition, we define *in-closeness centrality* as the reciprocal of the average cost of weights of the shortest paths *ending* in a node. Recall that the cost of an edge within a shortest path is the reciprocal of the directed link between two nodes. Nodes with high in-closeness centrality are therefore lying at the end of production paths with heavy global flows. In-closeness also does not subsume the effect of CPV on future stock returns (specification (4)).

We extend the horse-race with measures of foreign influence. First, we consider *weighted outdegree*, which sums all edges outgoing from a node. The measure is analogous to weighted indegree and captures the direct impact of an economy-industry pair on its customers. We also define *out-closeness centrality* as the reciprocal of the average sum of costs of the shortest paths *originating* from a node. Thus, nodes with high out-closeness centrality are economy-industry pairs important as suppliers for downstream consuming industries. Similarly to betweeness centrality, some of the top economy-industry pairs with high out-closeness centrality include

the Wholesale and Retail industries (e.g. USA and China). This reflects the importance of commoddity suppliers in the global production network. The measure also captures the importance of crude-oil producing countries, such as Russia and Saudi Arabia. The two measures of influence are naturally closely related, with a correlation of 0.92. The results in the last two specifications of Table 10 show that CPV is a stronger predictor of future performance than the measure of foreign influence.

5.6 Average Centrality as Predictor of Performance

As an alternative to betwenness centrality, we construct a measure of choke points that takes into account the importance of nodes as a) bridges in connecting other nodes, as well as their impact on b) nodes downstream, and c) nodes upstream. To this end, we compute *average centrality* as the average of betweenness centrality, out-closeness centrality and in-closeness centrality. Average centrality therefore recognizes that within global production networks, productivity shocks may also propagate downstream from important suppliers and upstream from important consumers. This measure is positively correlated with all measures of centrality reported in Table A1 of Appendix C. Thus, average centrality captures common information with all measures that identify systematically important nodes. We report the performance of portfolios sorted on average centrlaity in Table 11, using the same performance evaluation methods as in the CPV sorts. We find that similar to CPV, average centrality contains predictive power about the future performance of economy-industry pairs. However, the patterns are less monotonic, indicating that CPV is a stronger predictor of future performance, consistent with the analysis in Table 10.

5.7 Returns Using Lagged Choke Point Values

One potential caveat with our pricing tests is that we use the most recent production network to construct centrality. Naturally, there would be a delay before the data on global trade becomes public or before market participants are able to infer the choke points using alternative data. We therefore replicate the univariate portfolio sorts using a lagged CPV instead of the most-recently available one. Results are summarized in Table 12. We report the excess returns and abnormal returns from various asset pricing models for the low and high portfolio, as well as for the spread portfolio. We find results consistent with those in Table 7. The abnormal return

of the spread portfolio remains statistically different from zero across all asset pricing models.

6 Conclusion

The structure of the global supply chain and its evolution over time have caught much attention since the global pandemic. In this paper, we study the dynamic structure of global production networks and the implications for asset prices. Using world input-output tables to build global production networks, we propose a novel measure that identifies choke points based on the importance of an economy's industry in bridging global production networks. That is, shocks to a choke point can disrupt global production networks. We find that the choke points tend to locate relatively upstream in economies with better educated labor force, more developed capital markets, better governance, and deep seaports. Following the accession of China into the WTO, a rising number of choke points migrate out of the US, into China.

Using the recent Houthi attacks on container ships in the Red Sea and its subsequent blockage, we study how shocks to choke points propagate in the production network. We find strong evidence of the negative shock propagating from central Water Transport industries, affected by the Houthi attacks, to connected industries. Finally, we find that in global stock markets, firms in the choke points outperform by more than 6% per year. The higher stock returns on these firms tend to be persistent, which lends support to the view that the global stock markets tend to perceive them as riskier, thereby commanding a higher risk premium.

References

Acemoglu, D., Akcigit, U., and Kerr, W. (2016). Networks and the macroeconomy: An empirical exploration. *NBER Macroeconomics Annual*, 30:273–335.

Acemoglu, D., Carvalho, V. M., Ozdaglar, A., and Tahbaz-Salehi, A. (2012). The network origins of aggregate fluctuations. *Econometrica*, 80(5):1977 – 2016.

Acemoglu, D. and Tahbaz-Salehi, A. (2024). The macroeconomics of supply chain disruptions. *The Review of Economic Studies*, pages 1–40.

Ahern, K. (2013). Network centrality and the cross section of stock returns. *Working Paper*.

Antràs, P. (2023). An 'austrian' model of global value chains. Technical report, National Bureau of Economic Research.

Antràs, P. and Chor, D. (2021). Global value chains. Working Paper 28549, National Bureau of Economic Research.

Antràs, P., Chor, D., Fally, T., and Hillberry, R. (2012). Measuring the upstreamness of production and trade flows. *American Economic Review*, 102(3):412–16.

Baldwin, R. and Freeman, R. (2022). Risks and global supply chains: What we know and what we need to know. *Annual Review of Economics*, 14(Volume 14, 2022):153–180.

Baqaee, D. and Rubbo, E. (2023). Micro propagation and macro aggregation. *Annual Review of Economics*, 15(Volume 15, 2023):91–123.

Barabási, A.-L. and Pósfai, M. (2016). *Network science*. Cambridge University Press.

Barrot, J.-N., Loualiche, E., and Sauvagnat, J. (2019). The globalization risk premium. *The Journal of Finance*, 74(5):2391–2439.

Barrot, J.-N. and Sauvagnat, J. (2016). Input specificity and the propagation of idiosyncratic shocks in production networks *. *The Quarterly Journal of Economics*, 131(3):1543–1592.

Bekaert, G., Hodrick, R. J., and Zhang, X. (2009). International stock return comovements. *The Journal of Finance*, 64(6):2591–2626.

Bonacich, P. (1987). Power and centrality: A family of measures. *American Journal of Sociology*, 92(5):1170–1182.

Borgatti, S. P. (2005). Centrality and network flow. *Social Networks*, 27(1):55–71.

Brandes, U. (2001). A faster algorithm for betweenness centrality*. *The Journal of Mathematical Sociology*, 25(2):163–177.

Brandt, L., Van Biesebroeck, J., Wang, L., and Zhang, Y. (2017). Wto accession and performance of chinese manufacturing firms. *American Economic Review*, 107(9):2784–2820.

Carvalho, V. M., Nirei, M., Saito, Y. U., and Tahbaz-Salehi, A. (2021). Supply chain disruptions: Evidence from the great east japan earthquake*. *The Quarterly Journal of Economics*, 136(2):1255–1321.

Carvalho, V. M. and Tahbaz-Salehi, A. (2019). Production networks: A primer. *Annual Review of Economics*, 11(Volume 11, 2019):635–663.

Cohen, L. and Frazzini, A. (2008). Economic links and predictable returns. *The Journal of Finance*, 63(4):1977–2011.

Council of Economic Advisers (2022). Annual Report of the Council of Economic Advisers. Report Trasmitted to Congress, available at: `https://www.whitehouse.gov/wp-content/uploads/2022/04/ERP_2022_.pdf`.

Dijkstra, E. (1959). A note on two problems in connexion with graphs. *Numerische Mathematik*, 1:269–271.

Elliott, M., Golub, B., and Leduc, M. V. (2022). Supply network formation and fragility. *American Economic Review*, 112(8):2701–47.

Elliott, M. and Jackson, M. O. (2024). Supply Chain Disruptions, the Structure of Production Networks, and the Impact of Globalization. Working Paper, available at: `https://ssrn.com/abstract=4580819`.

Erten, B. and Leight, J. (2021). Exporting Out of Agriculture: The Impact of WTO Accession on Structural Transformation in China. *The Review of Economics and Statistics*, 103(2):364–380.

Freeman, L. C. (1977). A set of measures of centrality based on betweenness. *Sociometry*, 40(1):35–41.

Freeman, L. C., Borgatti, S. P., and White, D. R. (1991). Centrality in valued graphs: A measure of betweenness based on network flow. *Social Networks*, 13(2):141–154.

Gofman, M., Segal, G., and Wu, Y. (2020). Production Networks and Stock Returns: The Role of Vertical Creative Destruction. *The Review of Financial Studies*, 33(12):5856–5905.

Grossman, G. M., Helpman, E., and Lhuillier, H. (2023). Supply chain resilience: Should policy promote international diversification or reshoring? *Journal of Political Economy*, 131(12):3462–3496.

Herskovic, B. (2018). Networks in production: Asset pricing implications. *The Journal of Finance*, 73(4):1785–1818.

Hummels, D., Ishii, J., and Yi, K.-M. (2001). The nature and growth of vertical specialization in world trade. *Journal of International Economics*, 54(1):75–96.

Jensen, T. I., Kelly, B., and Pedersen, L. H. (2023). Is there a replication crisis in finance? *The Journal of Finance*, 78(5):2465–2518.

Johnson, R. C. and Noguera, G. (2017). A portrait of trade in value-added over four decades. *Review of Economics & Statistics*, 99(5):896 – 911.

Katz, L. (1953). A new status index derived from sociometric analysis. *Psychometrika*, page 39–43.

Kim, S.-J. and Shin, H. (2023). Theory of Supply Chians: A Working Capital Approach. Wroking Paper, available at: `https://papers.ssrn.com/sol3/papers.cfm?abstract_id=4361026`.

Kinney, R., Crucitti, P., Albert, R., and Latora, V. (2005). Modeling cascading failures in the north american power grid. *The European Physical Journal B-Condensed Matter and Complex Systems*, 46(1):101–107.

Koijen, R. S. J. and Yogo, M. (2019). A demand system approach to asset pricing. *Journal of Political Economy*, 127(4):1475–1515.

Lane, J. M. and Pretes, M. (2020). Maritime dependency and economic prosperity: Why access to oceanic trade matters. *Marine Policy*, 121:104180.

Leontief, W. (1986). *Input-Output Economics*. Oxford University Press.

Lund, S., Manyika, J., Woetzel, J., Ed Barriball and, Washington, D. M. K., Alicke, K., Birshan, M., George, K., Smit, S., Swan, D., and Hutzler, K. (2020). Risk, Resilience, and Rebalancing in Global Value Chains. McKinsey Global Institute Report.

Menzly, L. and Ozbas, O. (2010). Market segmentation and cross-predictability of returns. *The Journal of Finance*, 65(4):1555–1580.

Newman, M. E. J. (2001). Scientific collaboration networks. ii. shortest paths, weighted networks, and centrality. *Phys. Rev. E*, 64:016132.

Opsahl, T., Agneessens, F., and Skvoretz, J. (2010). Node centrality in weighted networks: Generalizing degree and shortest paths. *Social Networks*, 32(3):245–251.

Ramírez, C. A. (2024). Firm networks and asset returns. *The Review of Financial Studies*, 37(10):3050–3091.

The White House (2021). Building Resilient Supply Chains, Revitalizing American Manufacturing, and Fostering Broad-Based Growth. Report, available at: `https://www.whitehouse.gov/wp-content/uploads/2021/06/100-day-supply-chain-review-report.pdf`.

Table 1: Descriptive Statistics of the Global Production Network

This table presents summary statistics for the Global Production Network, based on OECD's Trade in Value Added (TiVA) between 1995 and 2020. A directed edge connects two nodes $n(r,i)$ and $n(s,j)$ and is equal to the value added by industry r in economy i to industry s in economy j, i.e. $FVA_{i,j}^{r,s}$ (in percentages). Note that since $FVA_{i,j}^{r,s} = 0$ if $i = j$, all edges linking industries from the same economy are set to 0. Each year we compute a mean and a standard deviation for all incoming and outgoing edges. We present the averages of the mean and standard deviations across all years, as well as global minimum and maximum values. We present the summary statistics for all nodes and for nodes belonging to geographical regions and sectors. Developed Asia-Pacific (APA) includes AUS, HKG, JPN, NZL, and SGP; Developed Europe (EUR) includes AUT, BEL, CHE, DEU, DNK, ESP, FIN, FRA, GBR, GRC, IRL, ITA, LUX, NLD, NOR, PRT, and SWE; Developed North-America (NAM) includes CAN and USA; Emerging and Frontier Asia-Pacific (APA) includes BGD, CHN, IDN, IND, KHM, KOR, LAO, MMR, MYS, PAK, PHL, THA, TWN, and VNM; Emerging and Frontier Europe (EUR) includes BGR, BLR, CYP, CZE, EST, HRV, HUN, ISL, LTU, LVA, MLT, POL, ROU, RUS, SVK, SVN, TUR, and UKR; Emerging and Frontier Latin America (LAM) includes ARG, BRA, CHL, COL, CRI, MEX, and PER; the Res of the World (ROW) includes BRN, CIV, CMR, EGY, ISR, JOR, KAZ, MAR, NGA, ROW, SAU, SEN, TUN, and ZAF. The sectors breakdown includes Agriculture, Forestry and Fishing (AGR), Mining and Quarrying (MIN), Manufacturing (MAN), Electricity, Gas, Water Supply, Sewerage, Waste and Remediation Services (UTL), Construction (CON), Total Business Sector Services (BUS), and all other (OTH) including Public Admin, Education and Health, and Social and Personal Services.

	ALL	Region							Sector						
		Developed			Emerging and Frontier										
		APA	EUR	NAM	APA	EUR	LAM	ROW	AGR	MIN	MAN	UTL	CON	BUS	OTH
Economies	77	5	17	2	14	18	7	14	77	77	77	77	77	77	77
Industries	45	45	45	45	45	45	45	45	2	3	17	2	1	14	6
Nodes:															
Econ-Ind Pairs	3465	225	765	90	630	810	315	630	154	231	1309	154	77	1078	462
Edges IN:															
Mean	0.006	0.006	0.006	0.004	0.006	0.007	0.004	0.005	0.005	0.005	0.009	0.004	0.005	0.005	0.003
StDev	0.071	0.069	0.070	0.056	0.071	0.083	0.055	0.063	0.039	0.051	0.100	0.087	0.032	0.044	0.021
Min	0	0	0	0	0	0	0	0	0	0	0	0	0	0	0
Max	72.15	31.33	41.21	12.80	37.79	49.72	24.75	72.15	11.11	20.00	72.15	37.41	6.99	20.40	12.25
Edges OUT:															
Mean	0.006	0.007	0.010	0.028	0.005	0.003	0.002	0.004	0.003	0.013	0.005	0.004	0.002	0.009	0.001
StDev	0.071	0.051	0.059	0.132	0.039	0.074	0.023	0.104	0.030	0.222	0.043	0.021	0.008	0.055	0.004
Min	0	0	0	0	0	0	0	0	0	0	0	0	0	0	0
Max	72.15	9.79	41.21	24.39	18.27	49.72	22.09	72.15	11.11	72.15	23.84	6.37	0.72	20.40	3.55

Table 2: Descriptive Statistics of Choke Point Values

This table presents summary statistics for our measure of Choke Point Values, computed as betweenness centrality between 1995 and 2020 (see Section 3) We present averages of the mean and standard deviations across all years, as well as global minimum and maximum values. We present summary statistics for all nodes and for nodes belonging to geographical regions and sectors as defined in Table 1. In Panel A, we present summary statistics for the whole sample, and in Panel B we present summary statistics for the economy-industry pairs with sufficient financial data to be included in our asset-pricing tests.

	ALL	Region							Sector						
		Developed			Emerging and Frontier										
		APA	EUR	NAM	APA	EUR	LAM	ROW	AGR	MIN	MAN	UTL	CON	BUS	OTH
	Panel A: All 3465 Economy-Industry Pairs														
Choke Point Index:															
Mean	0.007	0.010	0.012	0.027	0.006	0.005	0.002	0.003	0.002	0.006	0.010	0.001	0.001	0.007	0.000
StDev	0.040	0.059	0.055	0.066	0.043	0.018	0.008	0.021	0.007	0.037	0.045	0.004	0.005	0.047	0.002
Min	0	0	0	0	0	0	0	0	0	0	0	0	0	0	0
Max	1	1	1	1	1	0.52	0.20	0.85	0.08	0.85	1	0.12	0.14	1	0.06
	Panel B: All Economy-Industry Pairs with Financial Data														
#Economies	41	4	12	2	11	3	3	6	3	8	23	9	20	41	5
#Industries	41	35	27	39	34	7	3	8	1	3	17	2	1	13	4
#Econ-Ind Pairs	358	73	78	55	122	10	5	15	3	15	145	11	20	154	10
Choke Point Index:															
Mean	0.030	0.028	0.023	0.042	0.033	0.001	0.000	0.004	0.005	0.027	0.047	0.005	0.000	0.021	0.001
StDev	0.101	0.107	0.051	0.086	0.125	0.001	0.001	0.009	0.002	0.048	0.126	0.008	0.001	0.086	0.002
Min	0	0	0	0	0	0	0	0	0	0	0	0	0	0	0
Max	1	1	1	1	1	0.02	0.01	0.18	0.02	0.35	1	0.12	0.01	1	0.02

Table 3: The Determinants of Choke Points

This table presents the results of OLS regressions of Choke Point Value on lagged economy characteristics. The dependent variable in each regressions is log of one plus unstandardized betweenness centrality, computed for economy-industry pairs between 1997 and 2020 (see Section 3). We begin the analysis in 1997 due to the availability of data. The control variables include four lagged variables measuring different aspects of economic development, all standardized cross-sectional to have a mean of zero and unit variance: $GOVERNANCE$, computed as the average of the World Governance Indicators (including Control of Corruption, Governance Effectiveness, Political Stability and Absence of Violence, Regulatory Quality, Rule of Law, and Voice and Accountability), $log(EDUCATION)$, computed as the log of the percentage of population with tertiary education, $log(MCAPtoGDP)$, computed as log of the market capitalization of listed domestic companies in percentage of GDP. $AVE\ DEVELOPMENT$ is the average across all the economic development indicators with present data. $DEEP\ PORTS$ is computed as the number of ports with cargo water depth of at least 30 feet at the docking area that are used to dock, load, and unload cargo from large ocean freight vessels and river barges, also standardized to have a mean of zero and unit variance. We further include log of population ($log(POPULATION)$), yearly change in GDP per capital ($\Delta GDPHEAD$), yearly change in inflation ($\Delta INFL$), the yearly return of the currency against the US dollar ($FX\ RET$, in bp), yearly average of short-term interest rates (IR) and upstreamness ($UPSTREAMNESS$, defined in Appendix C). All independent variables are measured at the end of the previous year and all specifications include year fixed effects. t-statistics are given in parentheses, based on standard errors clustered on the economy level. Statistical significance at the 10%, 5%, and 1% level is indicated by *, **, and ***, respectively.

	(1)	(2)	(3)	(4)	(5)	(6)	(7)
$GOVERNANCE$	0.933***						
	(5.36)						
$log(EDUCATION)$		0.601***					
		(3.31)					
$log(MCAP\ TO\ GDP)$			0.493**				
			(2.13)				
$AVE\ DEVELOPMENT$				0.964***	0.785***	0.660**	0.469*
				(4.88)	(4.06)	(2.06)	(1.69)
$DEEP\ PORTS$					0.546***	0.397**	0.468**
					(4.06)	(2.12)	(2.58)
$log(POPULATION)$						0.090	0.074
						(0.56)	(0.47)
$\Delta GDPHEAD$						0.740	−0.376
						(0.23)	(−0.13)
$\Delta INFL$						0.487	1.124
						(0.18)	(0.44)
$FX\ RET$						−0.340	−0.358
						(−1.36)	(−1.46)
IR						−0.041*	−0.041*
						(−1.78)	(−1.87)
$UPSTREAMNESS$							1.767***
							(12.51)
Time FE	YES	YES	YES	YES	YES	YES	YES
Observations	82,004	39,423	60,474	82,004	82,004	59,890	59,890
R-squared	0.046	0.018	0.014	0.039	0.053	0.043	0.147

Table 4: The Impact of China's WTO Accession on the Importance of China and the USA as Choke Points

This table presents the results of OLS regressions of the impact of China's WTO accession in 2001 on economy-level Choke Point Values. The dependent variable in each regressions is log of one plus unstandardized economy-level betweenness centrality, computed for all countries between 1997 and 2020 (see Section 3). We begin the analysis in 1997 due to the availability of data. We include indicator variables for China and the USA (I^{CHN} and I^{USA}), as well as their interactions with an indicator variable for the post-2001 period ($I^{POST\ 2001}$). All other variables are defined in Table 3. All specifications include year fixed effects. t-statistics are given in parentheses, based on standard errors clustered on the economy level. Statistical significance at the 10%, 5%, and 1% level is indicated by *, **, and ***, respectively.

	(1)	(2)	(3)	(4)
I^{CHN}	0.950***		0.986***	1.058**
	(6.05)		(6.36)	(2.12)
$I^{CHN} * I^{POST\ 2001}$	1.238***		1.231***	0.831***
	(18.35)		(18.10)	(4.66)
I^{USA}		2.696***	2.709***	0.491
		(17.57)	(17.48)	(1.16)
$I^{USA} * I^{POST\ 2001}$		−0.601***	−0.584***	−0.300***
		(−8.70)	(−8.60)	(−3.67)
$AVE\ DEVELOPMENT$				0.617***
				(3.47)
$DEEP\ PORTS$				0.210
				(1.56)
$log(POPULATION)$				0.060
				(0.54)
$\Delta GDPHEAD$				1.008
				(0.47)
$\Delta INFL$				2.067
				(0.82)
$FX\ RET$				−0.154
				(−0.75)
IR				−0.040**
				(−2.44)
Time FE	YES	YES	YES	YES
Observations	2,002	2,002	2,002	1,332
R-squared	0.029	0.039	0.066	0.317

Table 5: Top 5 Affected Water Transport Industries Around the Houthi Attacks

This table presents key statistics for the five Water Transport industries, most affected by the Houthi attacks. We report CPV rank, total shortest paths passing via the node used to compute the CPV, the number of treated paths (computed as the total number of shortest paths between Asia and Developed Europe that pass through the water transportation industry, additionally requiring that the shortest path does not pass through North or South America), also expressed as a percentage of the total shortest paths passing via. All data is based on the 2020 global production network.

	DNK	GRC	SGP	CYP	NOR
CPV Rank	3	12	29	57	82
Total Shortest Paths Passing Via	1,800,144	615,224	295,417	184,332	130,010
Treated Shortest Paths	215,781	86,049	44,242	34,417	30,927
Percentage Affected Shortest Paths	12%	14%	15%	19%	24%

Table 6: Abnormal Stock Returns on Economy-Industry Pairs Around the Houthi Attacks

This table presents the results of OLS regressions of weekly economy-industry alphas on the fraction of all of the economy-industry pair's shortest paths affected by the Houthi's attacks. The dependent variable is weekly alpha, computed in two steps. In the first step over the period Oct 03, 2022 to Sep 29, 2023, for each economy-industry pair we regress its weekly excess returns on the weekly excess returns of the global market portfolio. In the second step over the four weeks prior and the four weeks after Dec 29, 2023, for each economy-industry pair we compute alphas as realized excess returns minus the product of the estimated beta and the realized weekly excess return of the market. For each economy-industry pair in Developed Europe and Developed and Emerging Asia, we compute the total number of treated paths as the the total number of shortest paths with either a source or a sink in that economy-industry pair that pass through any water transportation industry, additionally requiring that the shortest paths do not pass through any economy in North and South America. We assign a zero for all other economy-industry pairs. $log(Exposure)$ is computed as log of one plus the total number of treated paths divided by all the shortest paths with either a source or a sink in that economy-industry pair. $log(DirectLlink)$ is computed as log of the sum of all edges with a source (sink) the economy-industry pair and a sink (source) in treated Water Transport industries. $Post$ is an indicator variable equal to one for observations in 2024 and zero otherwise. The sample spans the last four weeks of 2023 and the first four weeks of 2024. β is the computed beta from the first stage of the weekly alpha estimation. All other variables are defined in Appendix B. All specifications include week fixed effects and depending on the specification, economy × sector fixed effects. t-statistics are given in parentheses, based on standard errors clustered on the economy-industry pair level. Statistical significance at the 10%, 5%, and 1% level is indicated by *, **, and ***, respectively.

	(1)	(2)	(3)	(4)	(5)
$log(Exposure)$	0.879	6.200**	6.188**	7.882*	
	(0.30)	(3.39)	(2.94)	(1.93)	
$Post \times log(Exposure)$		−10.683**	−10.528**	−10.573**	
		(−2.65)	(−2.63)	(−2.55)	
$log(DirectLink)$					0.046
					(0.71)
$Post \times log(DirectLink)$					−0.042
					(−0.46)
β			−0.220	−0.389	−0.400
			(−0.66)	(−1.77)	(−1.81)
$log(BookEquity)$			−0.088	−0.073	−0.086
			(−1.00)	(−1.22)	(−1.25)
$log(MarketEquity)$			0.076	0.064	0.069
			(1.07)	(0.98)	(1.04)
$Profitability$			0.559	−0.081	−0.042
			(1.14)	(−0.24)	(−0.12)
$Investment$			−0.085	−0.053	−0.066
			(−0.56)	(−0.34)	(−0.43)
$Dividends$			0.867	0.579**	0.513
			(1.47)	(2.37)	(1.87)
Ret^{m1}			3.612**	−0.064	−0.026
			(2.37)	(−0.08)	(−0.04)
$Ret^{m2:m12}$			−0.490	−1.273	−1.249
			(−0.79)	(−1.85)	(−1.83)
Time FE	Yes	Yes	Yes	Yes	Yes
economy × Sector FE	No	No	No	Yes	Yes
Observations	3,300	3,300	3,292	3,292	3,222
R-squared	0.064	0.070	0.082	0.166	0.159

Table 7: Choke Point Values and Stock Returns: Portfolio Analysis

This table reports the performance of industry portfolios conditional on their Choke Point Value. At the end of each year between 1995 and 2020, we sort economy-industry pairs with sufficient financial data into five portfolios, based on their Choke Point Value. Next, we track the value-weighted monthly returns of the portfolios during the next 12 months, after which we rebalance. In Panel A, we report time-series averages of excess returns. In Panel B, we report alphas and factor loadings from a global 6-factor Fama-French model, including Mrk-rf, SMB, HML, MOM, CMA, and RMW as factors. In Panel C, we report alphas from alternative models for the spread portfolio in the portfolio sorts. WCAPM stands for a World CAPM model with time-varying betas. For each economy-industry pair and each month, we first estimate loadings on a value-weighted market portfolio consisting of all stocks in Compustat uisng the previous 36 months. Next, we compute the economy industry's alpha as its observed return in excess of the estimated market loading times this month's market excess return. We value-weight alphas across all economy-industry pairs in the portfolio and report time-series averages. WLCAPM stands for a World-Local CAPM, where we compute alphas analogously to the WCAPM model with an additional local factor, again using time-varying betas. Local factors are computed as the value-weighted returns of all stocks across a local region, orthogonalized on the market portfolio. We assign countries to regions following the classification in Table 1. We also present alphas using alternative standard asset global pricing models, based on Fama-French factors. CAPM includes Mrk-rf as a sole factor, FF3 adds SMB and HML, FF4 augments FF3 with MOM and FF5 augments FF3 with CMA and RMW. Last, we report alphas using local Fama-French factors, where we assign each economy-industry pair to its closest local Fama-French set of factors. Next, for each economy-industry pair and each month, we first estimate loadings on the local factors. Next, we compute the economy industry's alpha as its observed return in excess of the estimated market loading times this month's realized factor returns. We value-weight alphas across all economy-industry pairs in the portfolio and compute time-series averages. t-statistics are given in parentheses. Statistical significance at the 10%, 5%, and 1% level is indicated by *, **, and ***, respectively.

	Panel A: Excess Returns					
	1 (low)	2	3	4	5 (high)	5 – 1
Ret-rf	0.163	0.516	0.399	0.700***	0.673**	0.510***
	(0.55)	(1.59)	(1.25)	(2.92)	(2.13)	(3.03)
	Panel B: Alphas and Loadings from a Global 6-Factor FF Model					
	1 (low)	2	3	4	5 (high)	5 – 1
Alpha	−0.396***	−0.064	−0.090	0.126*	0.206**	0.602***
	(−2.97)	(−0.48)	(−0.90)	(1.65)	(2.51)	(3.87)
Mrkt-rf	0.901***	0.957***	1.001***	0.907***	1.001***	0.101**
	(25.63)	(26.94)	(38.09)	(45.04)	(46.46)	(2.46)
SMB	0.439***	0.322***	−0.069	−0.123***	−0.013	−0.452***
	(6.57)	(4.76)	(−1.38)	(−3.22)	(−0.31)	(−5.80)
HML	0.011	−0.088	0.005	0.014	−0.002	−0.013
	(0.14)	(−1.13)	(0.09)	(0.32)	(−0.04)	(−0.14)
MOM	−0.028	0.001	0.016	−0.027	−0.009	0.019
	(−0.83)	(0.04)	(0.62)	(−1.37)	(−0.44)	(0.48)
CMA	0.025	−0.077	−0.201**	0.044	−0.304***	−0.329**
	(0.23)	(−0.70)	(−2.47)	(0.70)	(−4.55)	(−2.59)
RMW	−0.003	0.013	−0.214***	0.127**	−0.262***	−0.258**
	(−0.04)	(0.13)	(−3.04)	(2.36)	(−4.52)	(−2.35)
	Panel C: Alpha Spreads using Alternative Models					
	WCAPM	WLCAPM	FF Global Factor Models			
			CAPM	FF3	FF4	FF5
Alpha Spread	0.487***	0.219**	0.382**	0.447***	0.452***	0.612***
	(2.90)	(2.03)	(2.47)	(3.06)	(3.02)	(3.98)
		FF Local Factor Models				
		CAPM	FF3	FF4	FF5	FF6
Alpha Spread		0.263**	0.348***	0.373***	0.432***	0.456***
		(2.57)	(3.52)	(3.69)	(4.34)	(4.33)

Table 8: Choke Point Values and Stock Returns: Portfolio Analysis Using Double Sorts

This table reports the performance of industry portfolios double sorted on network betas or market equity and their Choke Point Values. At the end of each year between 1995 and 2020, we sort economy-industry pairs with sufficient financial data into three portfolios, based on $\beta^{Concentration}$ (Panel A), $\beta^{Sparsity}$ (Panel B), or their total market equity (Panel C). For each economy-industry pair, we estimate $\beta^{Concentration}$ ($\beta^{Sparsity}$) in a regression of annual changes in exports on Network Concentration (Network Sparsity) across the full sample. Next, we double sort each portfolio into three portfolios, based on their Choke Point Value (CPV). Next, we track the value-weighted monthly returns of the portfolios during the next 12 months, after which we rebalance. We report alphas from a 6 factor model, including Mrk-rf, SMB, HML, MOM, CMA, and RMW as factors. t-statistics are given in parentheses. Statistical significance at the 10%, 5%, and 1% level is indicated by *, **, and ***, respectively.

Panel A: Double Sorts on $\beta^{Concentration}$ and CPV

$\beta^{Concentration}$	CPV			
	1 (low)	2	3 (high)	3 – 1
1 (low)	−0.233	−0.147	0.339**	0.573***
	(−1.14)	(−0.95)	(2.58)	(2.72)
2	−0.025	0.142	0.038	0.062
	(−0.14)	(1.17)	(0.39)	(0.33)
3 (high)	−0.382***	−0.090	−0.009	0.374**
	(−2.85)	(−0.76)	(−0.12)	(2.24)
3 – 1	−0.149	0.057	−0.348**	
	(−0.73)	(0.30)	(−2.17)	

Panel B: Double Sorts on $\beta^{Sparsity}$ and CPV

$\beta^{Sparisty}$	CPV			
	1 (low)	2	3 (high)	3 – 1
1 (low)	−0.435***	−0.012	0.213**	0.649***
	(−3.23)	(−0.09)	(2.34)	(3.78)
2	−0.155	0.062	0.271***	0.426**
	(−1.04)	(0.61)	(2.80)	(2.48)
3 (high)	−0.160	−0.193	−0.090	0.071
	(−0.89)	(−1.05)	(−0.58)	(0.37)
3 – 1	0.275	−0.181	−0.303	
	(1.41)	(−0.93)	(−1.52)	

Panel C: Double Sorts on Market Cap and CPV

$MarketEquity$	CPV			
	1 (low)	2	3 (high)	3 – 1
1 (low)	0.003	0.001	0.151	0.147
	(0.02)	(0.01)	(0.82)	(0.83)
2	−0.244*	−0.068	−0.034	0.210
	(−1.82)	(−0.51)	(−0.24)	(1.40)
3 (high)	−0.273**	0.072	0.150**	0.423***
	(−2.19)	(1.04)	(2.05)	(2.93)
3 – 1	−0.276	0.071	−0.000	
	(−1.53)	(0.41)	(−0.00)	

Table 9: Choke Point Values and Stock Returns: Regression Analysis

This table reports the results of Fama-MacBeth regression of economy-industry returns on their lagged Choke Point Value and lagged predictors of performance. The dependent variable is a value-weighted economy-industry return, expressed in percentages. CPV^{PRCNTL} is the most recently available Choke Point Value, expressed as a percentile. Economy-level variables are defined in Table 3, and all other variables are defined in Appendix B. t-statistics based on Newey-West standard errors are given in parentheses. Statistical significance at the 10%, 5%, and 1% level is indicated by *, **, and ***, respectively.

	(1)	(2)	(3)	(4)	(5)
CPV^{PRCNTL}	0.004***	0.003**	0.003***	0.003**	0.002**
	(2.79)	(2.35)	(2.68)	(2.36)	(2.10)
β	−0.082	0.024	−0.229	−0.092	−0.147
	(−0.31)	(0.10)	(−1.05)	(−0.44)	(−0.59)
$log(BookEquity)$	0.031	0.012	0.066	0.044	0.014
	(0.35)	(0.14)	(0.93)	(0.83)	(0.33)
$log(MarketEquity)$	−0.038	0.008	−0.062	−0.092	−0.062
	(−0.39)	(0.09)	(−0.90)	(−1.48)	(−1.19)
$Profitability$		0.043	0.043	0.021	0.001
		(0.29)	(0.37)	(0.19)	(0.01)
$Investment$		−0.060	−0.058	−0.041	−0.027
		(−1.28)	(−1.49)	(−1.28)	(−0.94)
$Dividends$		0.087	0.006	0.067	0.072
		(0.22)	(0.02)	(0.21)	(0.24)
Ret^{m1}			2.098	2.286*	1.668
			(1.50)	(1.85)	(1.37)
$Ret^{m2:m12}$			0.884	1.294***	1.196***
			(1.45)	(2.80)	(2.60)
$log(POPULATION)$				0.118**	0.115**
				(2.05)	(2.12)
$\Delta GDPHEAD$				−4.087	−6.614
				(−0.67)	(−1.12)
$\Delta INFL$				−1.041	−3.082
				(−0.34)	(−1.05)
$FX\ RET$				−0.026**	−0.023*
				(−2.14)	(−1.95)
$\beta^{Economy}$					0.168
					(0.60)
$\beta^{Concentration}$					−0.002
					(−0.81)
$\beta^{Sparsity}$					−0.003
					(−0.41)
β^{Transp}					0.229
					(0.76)
Observations	65,096	57,094	57,094	53,785	52,236
R-squared	0.143	0.184	0.260	0.375	0.422

Table 10: Centrality Measures and Stock Returns

This table reports the results of Fama-MacBeth regression of economy-industry returns on lagged measures of network centrality and lagged predictors of performance. The dependent variable is a value-weighted economy-industry return, expressed in percentages. All measures of network centrlality are defined in Appendix C and expressed as percentiles. In each specification, we include common predictors of performance (β, $log(BookEquity)$, $log(MarketEquity)$, $Profitability$, $Investment$, $Dividends$, Ret^{m1}, $Ret^{m2:m12}$), defined in Appendix B. t-statistics based on Newey-West standard errors are given in parentheses. Statistical significance at the 10%, 5%, and 1% level is indicated by *, **, and ***, respectively.

	(1)	(2)	(3)	(4)	(5)	(6)
CPV^{PRCNTL}	0.004***	0.004***	0.004***	0.004***	0.002*	0.002**
	(3.10)	(3.12)	(3.09)	(2.72)	(1.75)	(2.14)
$EIGEN^{PRCNTL}$	−0.002					
	(−0.79)					
KB^{PRCNTL}		−0.002				
		(−0.87)				
WIN^{PRCNTL}			−0.002			
			(−0.99)			
CLO_IN^{PRCNTL}				−0.002		
				(−0.92)		
$WOUT^{PRCNTL}$					0.002	
					(0.90)	
CLO_OUT^{PRCNTL}						0.001
						(0.73)
Controls	YES	YES	YES	YES	YES	YES
Observations	57,094	57,094	57,094	55,703	57,094	57,094
R-squared	0.271	0.271	0.271	0.271	0.270	0.268

Table 11: Average Centrality and Stock Returns: Portfolio Analysis

This table reports the performance of industry portfolios conditional on average centrality. At the end of each year between 1995 and 2020, we sort economy-industry pairs with sufficient financial data into five portfolios, based on their average Choke Point Value. Next, we track the value-weighted monthly returns of the portfolios during the next 12 months, after which we rebalance. In Panel A, we report time-series averages of excess returns, and alphas and factor loadings from a 6 factor model, including Mrk-rf, SMB, HML, MOM, CMA, and RMW as factors. In Panel B, we report alphas from alternative models. WCAPM stands for a World CAPM model with time-varying betas. For each economy-industry pair and each month, we first estimate loadings on a value-weighted market portfolio consisting of all stocks in Compustat. Next, we compute the economy industry's alpha as its observed return in excess of the estimated market loading times this month's market excess return. We value-weight alphas across all economy-industry pairs in the portfolio and report time-series averages. WLCAPM stands for a World-Local CAPM, where we compute alphas analogously to the WCAPM model with an additional local factor, again using time-varying betas. Local factors are computed as the value-weighted returns of all stocks across a local region, orthogonalized on the market portfolio. We assign countries to regions following the classification in Table 1. We also present alphas using alternative standard asset pricing models, based on Fama-French factors. CAPM includes Mrk-rf as a sole factor, FF3 adds SMB and HML, FF4 augments FF3 with MOM and FF5 augments FF3 with CMA and RMW. t-statistics are given in parentheses. Statistical significance at the 10%, 5%, and 1% level is indicated by *, **, and ***, respectively.

	Panel A: Excess Returns and 6F Alphas and Loadings					
Ret-rf	0.211	0.536**	0.475*	0.321	0.696**	0.486***
	(0.72)	(2.22)	(1.79)	(1.04)	(2.36)	(2.87)
Alpha	−0.345**	−0.133	−0.039	−0.041	0.153**	0.498***
	(−2.29)	(−1.23)	(−0.41)	(−0.47)	(2.23)	(2.99)
Mrkt-rf	0.850***	0.889***	0.950***	0.922***	1.008***	0.159***
	(21.42)	(31.16)	(38.48)	(39.58)	(56.06)	(3.62)
SMB	0.423***	0.105*	0.040	−0.040	−0.032	−0.455***
	(5.61)	(1.94)	(0.85)	(−0.91)	(−0.95)	(−5.47)
HML	0.107	−0.087	−0.094*	−0.023	0.073*	−0.034
	(1.23)	(−1.39)	(−1.73)	(−0.45)	(1.84)	(−0.36)
MOM	0.007	0.006	−0.011	−0.010	−0.010	−0.017
	(0.18)	(0.20)	(−0.45)	(−0.43)	(−0.57)	(−0.40)
CMA	−0.059	0.255***	0.120	−0.265***	−0.231***	−0.172
	(−0.48)	(2.87)	(1.56)	(−3.67)	(−4.14)	(−1.27)
RMW	0.031	0.290***	−0.129*	−0.376***	−0.114**	−0.146
	(0.30)	(3.78)	(−1.94)	(−6.01)	(−2.37)	(−1.24)

	Panel B: Alpha Spreads using Alternative Models					
	WCAPM	WLCAPM	FF Factor Models			
			CAPM	FF3	FF4	FF5
Alpha Spread	0.400**	0.245**	0.339**	0.390**	0.415***	0.489***
	(2.11)	(2.07)	(2.10)	(2.53)	(2.63)	(2.97)

Table 12: Lagged Choke Point Values and Stock Returns

This table reports the performance of industry portfolios conditional on their lagged Choke Point Values. At the end of each year between 1995 and 2020, we sort economy-industry pairs with sufficient financial data into five portfolios, based on lagged Choke Point Value. Next, we track the value-weighted monthly returns of the portfolios during the next 12 months, after which we rebalance. We report excess returns and alphas from several standard asset pricing models, based on Fama-French models, separately for the low Portfolio 1, the high Portflio 5, and the spread portfolio between Portfolios 5 and 1. CAPM includes Mrk-rf as a sole factor, FF3 adds SMB and HML, FF4 augments FF3 with MOM and FF5 augments FF3 with CMA and RMW, and FF6 includes all factors together. t-statistics are given in parentheses. Statistical significance at the 10%, 5%, and 1% level is indicated by *, **, and ***, respectively.

ExcRet	Alpha				
	CAPM	FF3	FF4	FF5	FF6
Portfolio 1 (low)					
0.231	−0.282**	−0.329**	−0.333**	−0.332**	−0.335**
(0.76)	(−2.01)	(−2.56)	(−2.53)	(−2.42)	(−2.41)
Portfolio 5 (high)					
0.648**	0.003	0.029	0.076	0.235***	0.251***
(2.03)	(0.03)	(0.34)	(0.86)	(2.74)	(2.90)
Portfolio 5 – 1					
0.417**	0.285*	0.358**	0.409**	0.567***	0.586***
(2.43)	(1.71)	(2.31)	(2.59)	(3.50)	(3.58)

Figure 3: Example Shortest Paths

This figure presents several shortest paths and direct paths in the global production network for 2020. The thickness of the line between two nodes represents the edge, labeled as percentage.

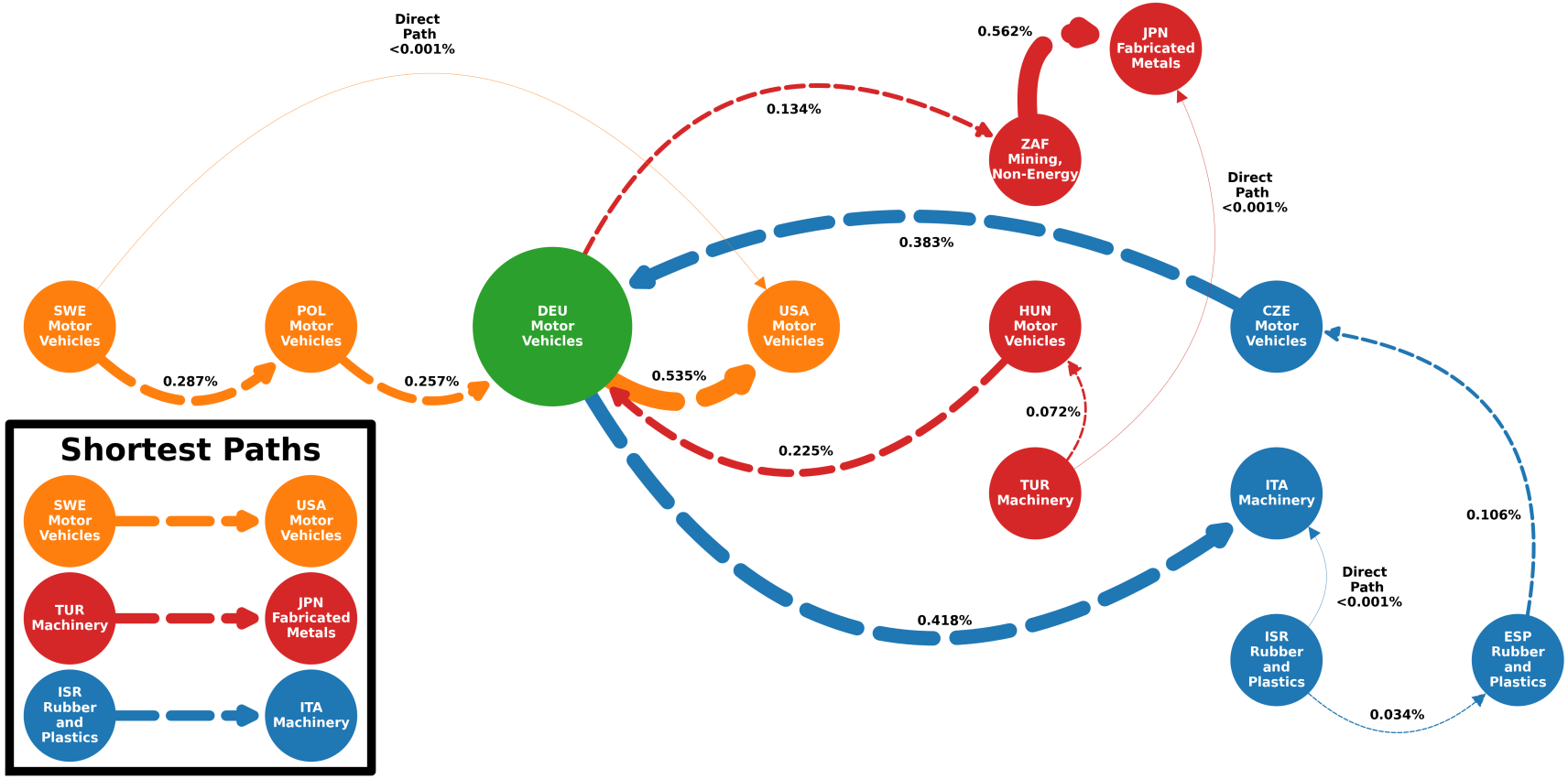


Figure 4: The Economy-Level Global Choke Points Network in 1995 and 2020

This figure presents a visual representation of the global network of choke points in 1995 (left side) and 2020 (right side), where each node is a economy. The thickness of the arrow from node A to node B represents the total number of shortest paths passing from node A to node B. The size of the node represents the total number of shortest paths passing via the node as a fraction of all shortest paths in the network, i.e., the economy's Choke Points Value (CPV). We label the CPV for all countries with CPV above 10%. We group countries into seven groups, based on the geography and economic development, following the classification in Table 1.

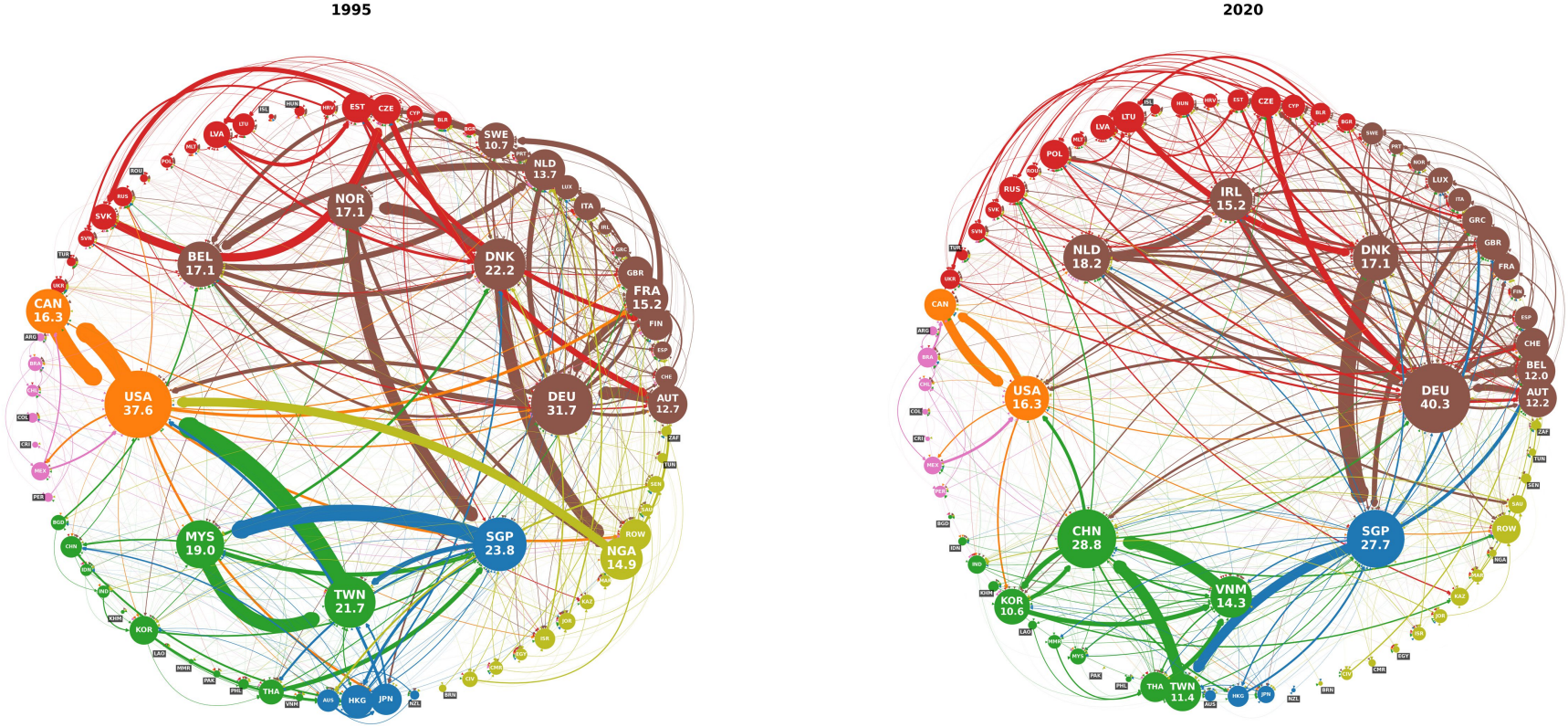


Figure 5: Top Countries and Industries with Highest Choke Point Values

This figure presents the top ten countries (Panel A) and top 10 industries (Panel B) with highest Choke Point Value in 1995 (left side) and 2020 (right side). The gray line track changes in the rank of countries and industries over time. The size of each bar represents the Choke Point Value, expressed in percentages.

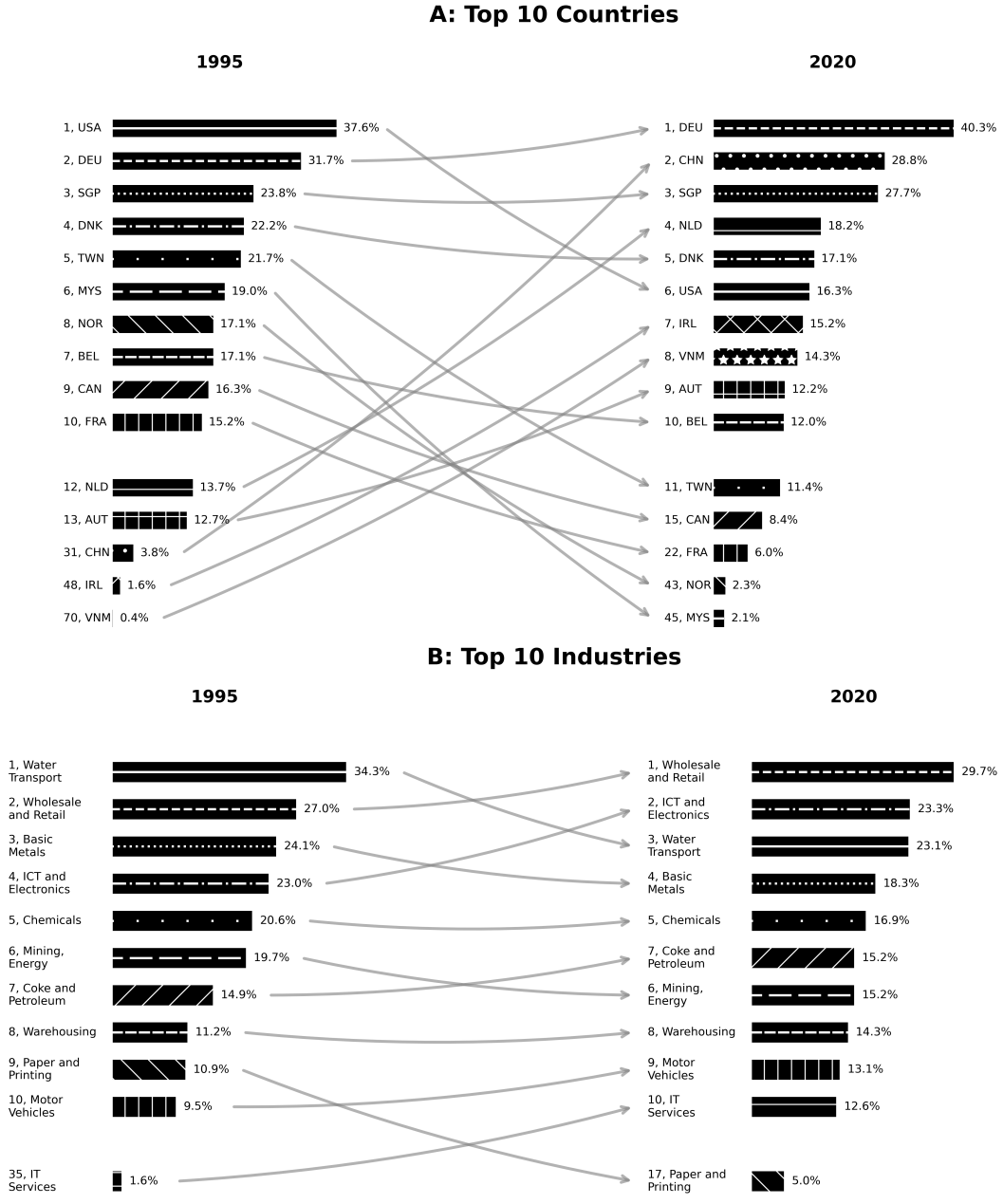
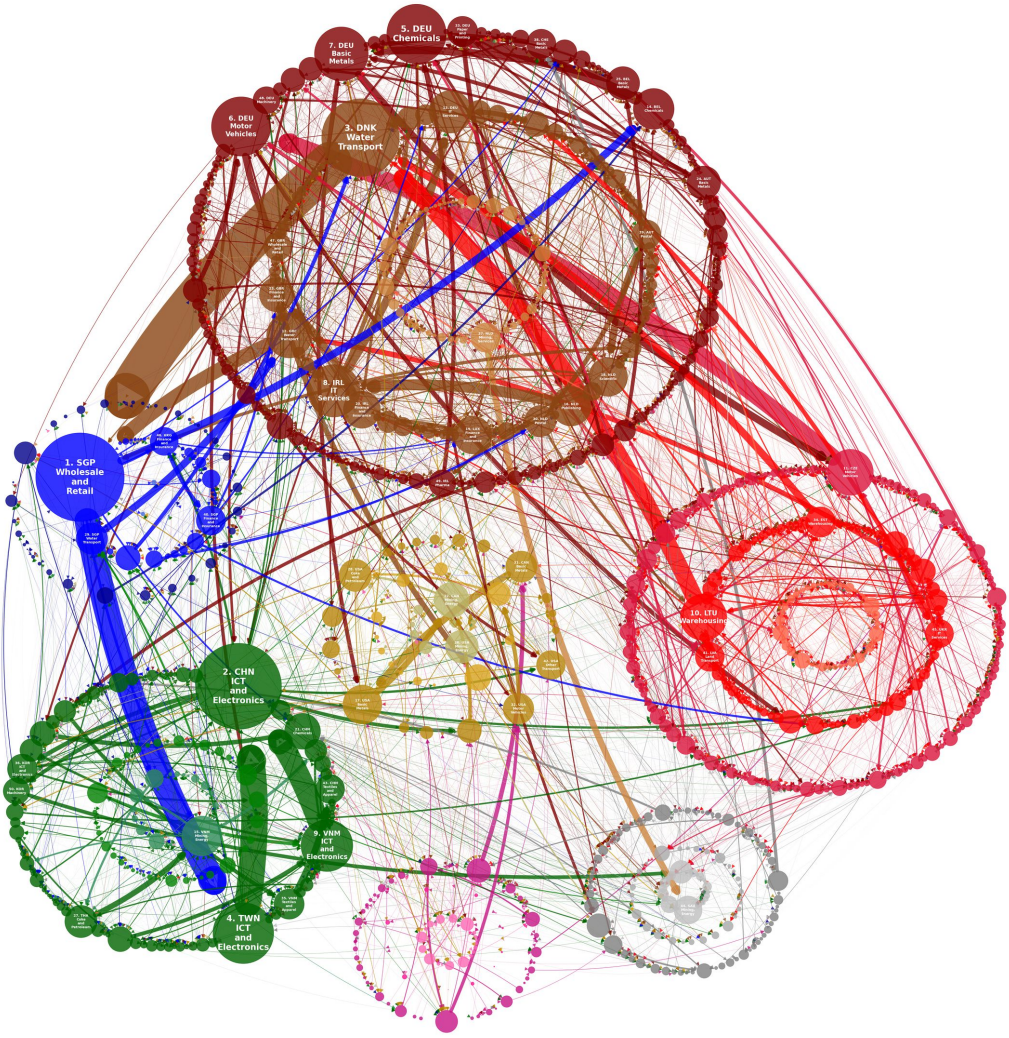


Figure 6: The Detailed Global Network of Choke Points in 2020

This figure presents a visual representation of the global network of choke points in 2020, where each node is an economy-industry pair. The thickness of the arrow from node A to node B represents the total number of shortest paths passing from node A to node B. The size of the node represents the total number of shortest paths passing via the node, i.e. the node's Choke Points Value. We group nodes into seven groups, based on the geography and economic development, following the classification in Table 1. Within each group of nodes, we place all manufacturing industries in the outer circle, all business services industries in the middle cirlce, and all other industries in the inner circle.



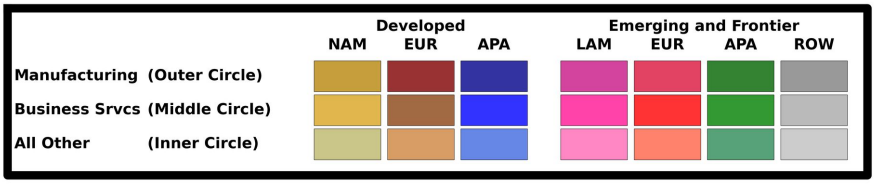


Figure 7: The Impact of China's WTO Accession on the Choke Point Vaue of China

This figure presents a visual representation of the global network of shortest paths passing via China before and after the its WTO accession in December 2001. The size of node China (in cyan, in the middle) represents the percentage of all shortest paths in the network passing via China, i.e., the economy's Choke Point Value. The thickness of the arrow from any of the other nodes represents the number of shortest paths originating from the source node that pass through China (label=out, expressed as a percentage of all shortest paths originating from the node). The thickness of the arrow from China to any target node represents the number of shortest paths from a source node that pass through China and end in the target node. The colors illustrate the flow of the shortest paths. For instance, color blue tracks shortest paths originating from Asia-Pacific Developed, passing via China, and ending in any node. We present the global network separately for the three years prior to the WTO accession (top row) and the three years subsequent to the WTO accession.

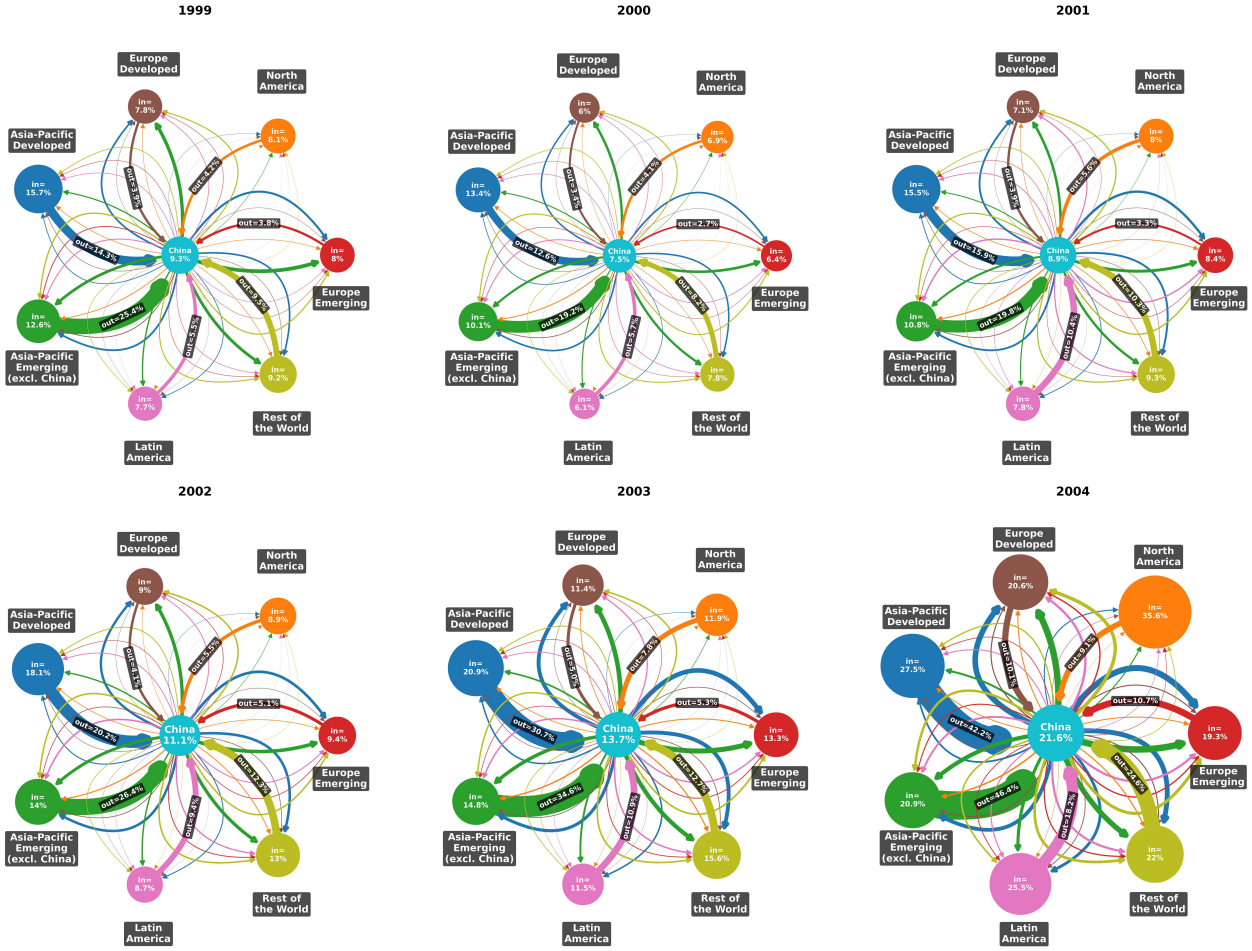


Figure 8: The Impact of China's WTO Accession on the Choke Point Value of the USA

This figure presents a visual representation of the global network of shortest paths passing via the USA before and after China's WTO accession in December 2001. The size of node USA (in cyan, in the middle) represents the percentage of all shortest paths in the network passing via USA, i.e. the economy's Choke Point Value. The thickness of the arrow from any of the other nodes represents the number of shortest paths originating from the source node that pass through USA (label=out, expressed as a percentage of all shortest paths originating from the node). The thickness of the arrow from USA to any target node represents the number of shortest paths from a source node that pass through USA and end in the target node. The colors illustrate the flow of the shortest paths. For instance, color blue tracks shortest paths originating from Asia-Pacific Developed, passing via USA, and ending in any node. We present the global network separately for the three years prior to the WTO accession (top row) and the three years subsequent to the WTO accession.

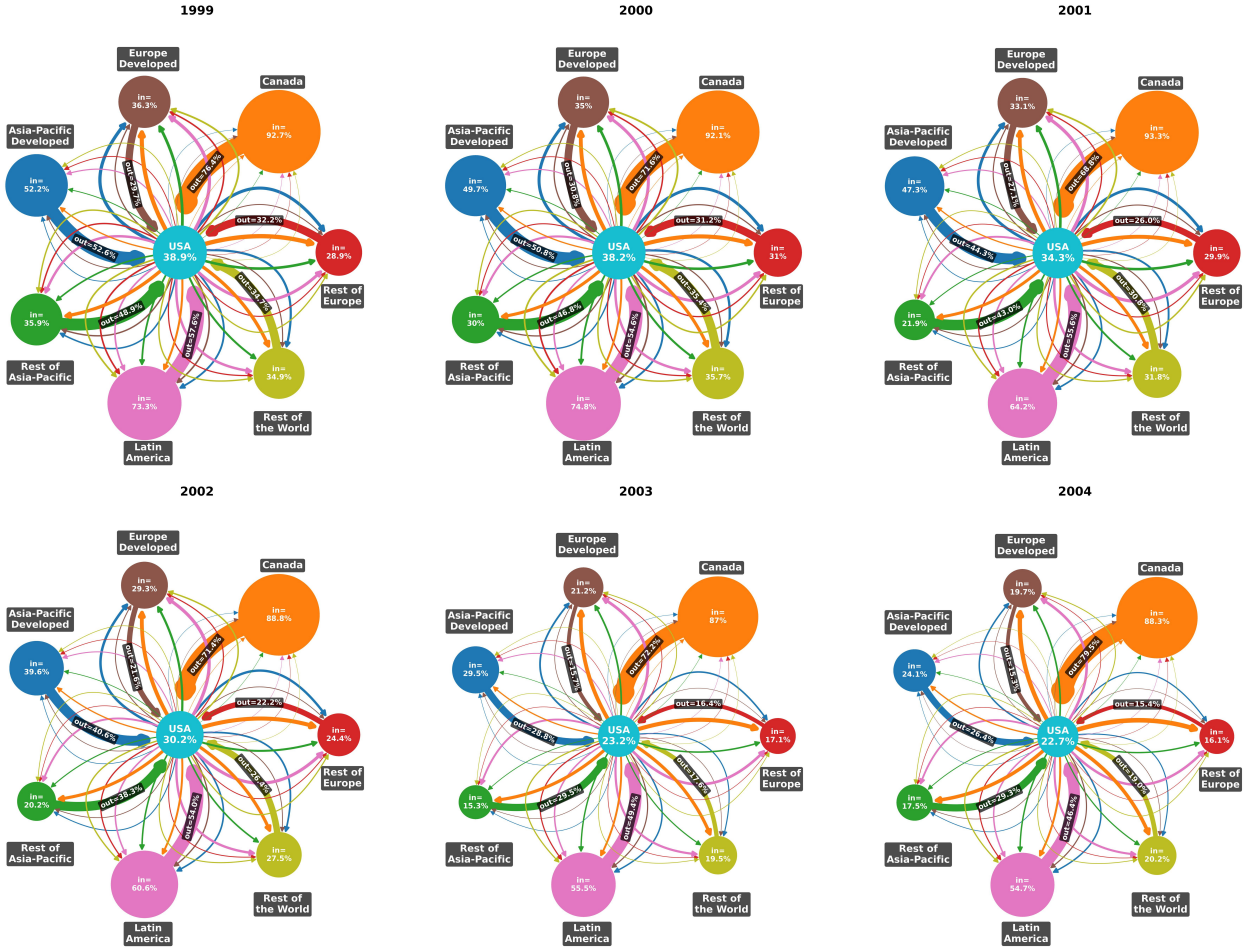


Figure 9: Daily Number of Container Shipis Passing via the Red Sea Around the Houthi Attacks

This figure presents the daily number of container ships in the Red Sea. The data comes from the Kiel Institute for the World Economy. The dashed line separates the before and after periods used for the regression analysis in Table 6.

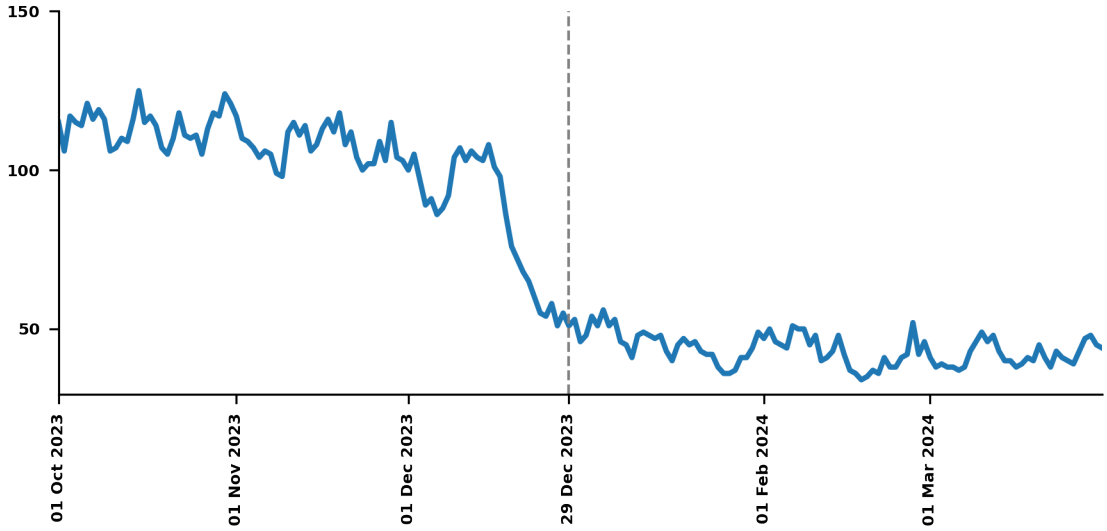


Figure 10: Container Price Index on the Far East to North Europe Trade Lane Around the Houthi Attacks

This figure presents an index on freight rates for less than 32 days for a standard 40' container on the trade lane between Far East and North Europe. The index is computed by Xeneta, using committed quotes reported by their customers. Xeneta computes dollar median rates for each Customer - Service Provider pair. The Index level is then computed as the weighted average of the median rates. (Refinitiv Code: *.XSICFENE*). The dashed line separates the before and after periods used for the regression analysis in Table 6.

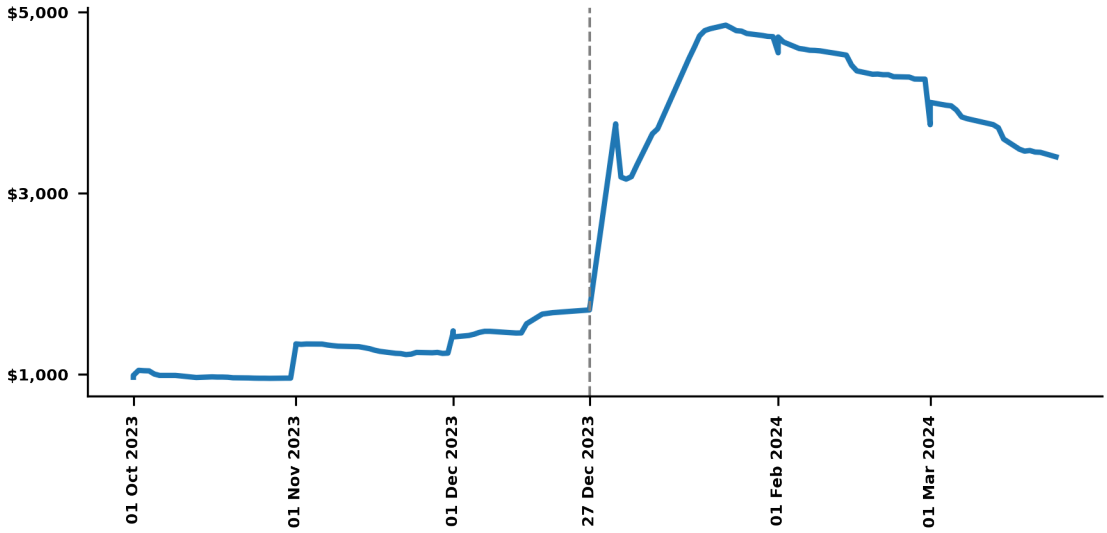


Figure 11: Propagation of the Shock to Water Transport in the Red Sea Across the World

This figure depicts the propagation of the shock to Water Transport industries using connecting shortest paths between Developed Europe and Developed and Emerging Asia-Pacific propagated. For each economy in Developed Europe and Developed and Emerging Asia, we compute the total number of treated paths as the the total number of shortest paths with either a source or a sink in that economy that pass through any Water Transport industry, additionally requiring that the shortest paths do not pass through any economy in North and South America. We express these as a fraction of all shortest paths with either a source or a sink in that economy ("Fraction of All Economy to Economy Shortest Paths, Affected by the Houthi Attacks"). Higher intensity of blue represents higher Fraction of All Economy to Economy Shortest Paths, Affected by the Houthi Attacks. All other countries are depicted in light gray. We label the 15 countries with highest values. The red dot represents the Bab el-Mandeb strait. The thickness of the solid arrows from the Bab el-Mandeb strait to any other economy represent the number of shortest paths connecting the strait with that economy. The thickness of the dashed arrows represent the directional number of shortest paths passing in that direction. For example, the thickness of the arrow labeled "Singapore → Taiwan" represents the number of shortest paths passing via Singapore in the direction of Taiwan that eventually sink in another economy.

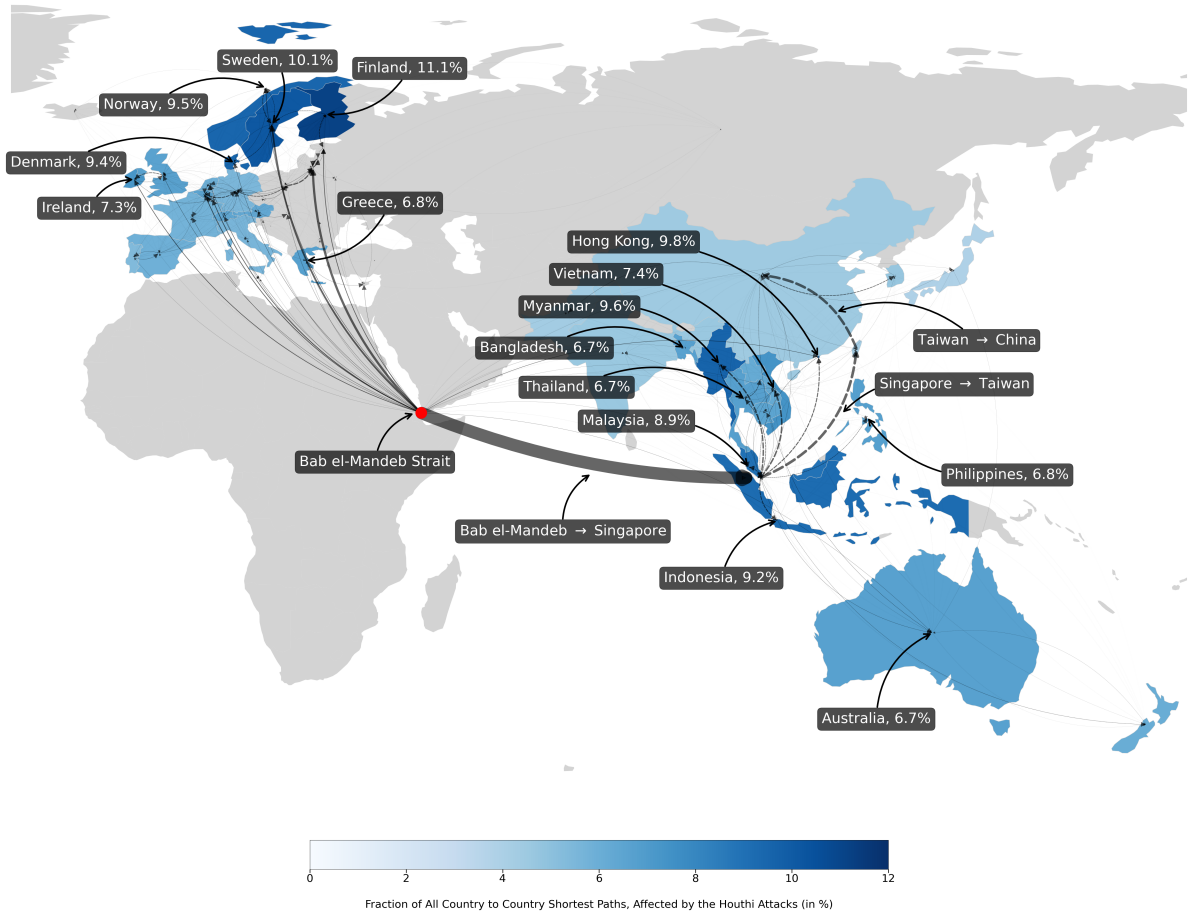
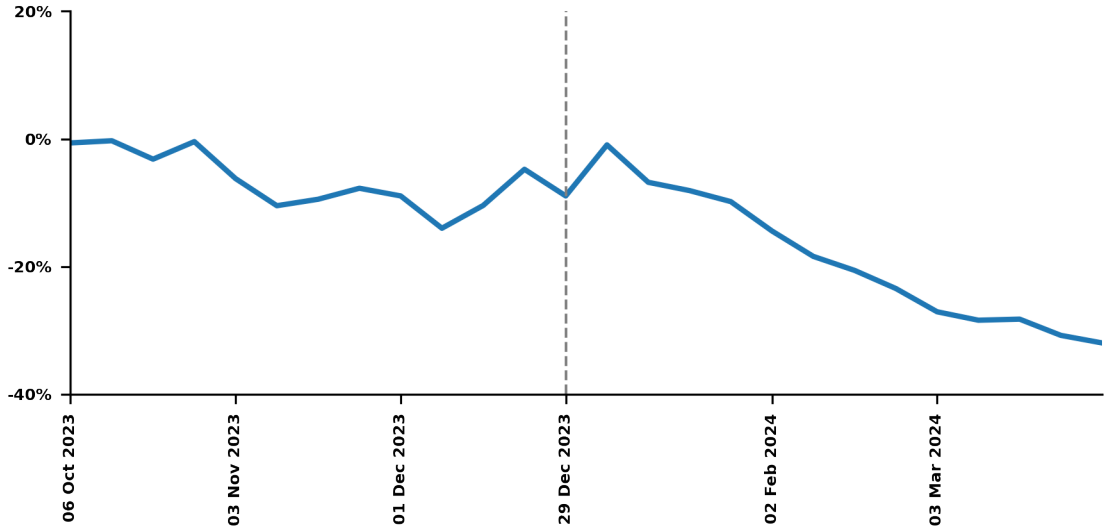


Figure 12: Cumulative Alpha of Companies in the Top Five Affected Water Industries by the Houthi Attacks

This figure presents the cumulative alpha of companies in the top 5 affected Water Transport industries around the Houthi attacks. We first select all stocks in the selected industries. We next compute stock weekly alphas in two steps. In the first step over the period Oct 03, 2022 to Sep 29, 2023, for each stock we regress its weekly excess returns on the weekly excess returns of the global market portfolio. In the second step and starting from October 2023, for each stock we compute abnormal alphas as realized excess returns minus the product of the estimated beta and the realized weekly excess return of the market. We plot the cumulative value of the weekly value-weighted alpha average between the beginning of October 2023 and end of March 2024. The dashed line separates the before and after periods used for the regression analysis in Table 6.



Online Appendices

Appendix A Unpacking the Sources of Value-Added in Global Value Chains

We provide an example WIOT in Figure A.1. The Table contains a matrix $\mathbf{Z}$ of size $JS \times JS$ (for example, $77 * 45 \times 77 * 45$ as in our WIOT from OECD). Each entry Z_{ij}^{rs} contains the value of inputs from industry r in economy i (row arrays) that is used by industry s in economy j (column arrays). Values of the output of each economy-industry pair that are instead absorbed in final-use, such as household consumption, are reported to the right of $\mathbf{Z}$. $\mathbf{F_j}$ is defined as a vector of size $JS \times 1$ that stacks the values F_{ij}^{r} of output from industry r in economy i that is absorbed in the final use of economy j. We denote the the sum of these vectors over all destination economies by $\mathbf{F} = \sum_j \mathbf{F_j}$.

The starting point for the value added decomposition is a basic gross output accounting identity. Define $\mathbf{Y}$ as the $JS \times 1$ vector of gross output values Y_j^s. Let $\mathbf{A}$ then be the $JS \times JS$ matrix of direct requirement coefficients, $a_{ij}^{rs} = Z_{ij}^{rs}/Y_j^s$ (value of the input from industry r in economy i that is used in the production of 1 dollar unit of output for industry s in economy j). The gross output of an economy-industry can then be expressed as:

$$\mathbf{Y} = \mathbf{F} + \mathbf{AY} = \mathbf{F} + \mathbf{AF} + \mathbf{A^2F} + \dots \tag{A.1}$$

Gross output is the sum of value absorbed in final use as well as the one purchased for use as an input from all other economy-industry pairs. We obtain the infinite sum representation by iteratively substituting for $\mathbf{F}$. According to this representation, the set of direct requirements coefficients in $\mathbf{A}$ describes the production technology, both when the output is used in final consumption or as an intermediary output (also irrespective of the destination economy).

Equation A.1 can be rewritten as

$$\mathbf{Y} = (\mathbf{I} - \mathbf{A})^{-1}\mathbf{F} \tag{A.2}$$

where where $\mathbf{I}$ is a $JS \times JS$ identity matrix and $(\mathbf{I} - \mathbf{A})^{-1}$ stands for the Leontieff inverse matrix

(Leontief, 1986).

From the WIOT, we can compute the part of the gross output that is exported abroad, stacked in vector $\mathbf{GX}$ of size $JS \times 1$. For example, for each economy i we can compute an $S \times 1$ vector of gross exports, with the r-th entry equal to $\sum_{j \neq i} \sum_s Z_{ij}^{rs} + \sum_{j \neq i} F_{ij}^r$. In the value-added decomposition, $\mathbf{V}$ is the $JS \times 1$ vector that is the transpose of the row vector of value-added entries VA_j^s. Each value-added entry represents the output of the economy-industry paper in excess of all inputs used, that is, $VA_j^s = Y_j^s - \sum_{i,r} Z_{ij}^{rs}$. Following Hummels et al. (2001), we can decompose the sources of value-added embedded in the gross exports by (i) taking the vector $\mathbf{GX}$ of gross exports for economy i; (ii) using the Leontief inverse $(\mathbf{I} - \mathbf{A})^{-1}$ to back out the gross output needed to generate this gross export vector; and then (iii) pre-multiplying this by a diagonal matrix of value-added shares in gross output, $\hat{\mathbf{V}}\hat{\mathbf{Y}}^{-1}$, where the 'hat' notation denotes a diagonal matrix whose main diagonal entries are the entries of the corresponding column vector.

$$\hat{\mathbf{V}}\hat{\mathbf{Y}}^{-\mathbf{1}}(\mathbf{I} - \mathbf{A})^{-1}\mathbf{GX} \tag{A.3}$$

The above expression results in a matrix of size $JS \times JS$ that decomposes gross exports into domestic and foreign sources of value-added and is commonly referred to as Trade in Value Added (TiVA). For an overview of the literature using WIOT analysis, see Antràs and Chor (2021).

Figure A.1: Standard World Input-Output Table

This figure presents a visual representation of a World Input-Output Table.

			Inputs Use and Value Added							Final Use			Total Use
			Economy 1			⋯	Economy J			Economy 1	⋯	Economy J	
			Industry 1	⋯	Industry S	⋯	Industry 1	⋯	Industry S				
Output	Economy 1	Industry 1	Z_{11}^{11}	⋯	Z_{11}^{1S}	⋯	Z_{1J}^{11}	⋯	Z_{1J}^{1S}	F_{11}^{1}	⋯	F_{1J}^{1}	Y_{1}^{1}
		⋯	⋯	Z_{11}^{rs}	⋯	⋯	⋯	Z_{1J}^{rs}	⋯	⋯	⋯	⋯	⋯
		Industry S	Z_{11}^{S1}	⋯	Z_{11}^{SS}	⋯	Z_{1J}^{S1}	⋯	Z_{1J}^{SS}	F_{11}^{S}	⋯	F_{1J}^{S}	Y_{1}^{S}
	⋯	⋯	⋯	⋯	⋯	⋯	⋯	⋯	⋯	⋯	⋯	⋯	⋯
Supplied	Economy J	Industry 1	Z_{J1}^{11}	⋯	Z_{J1}^{1S}	⋯	Z_{JJ}^{11}	⋯	Z_{JJ}^{1S}	F_{J1}^{1}	⋯	F_{JJ}^{1}	Y_{J}^{1}
		⋯	⋯	Z_{J1}^{rs}	⋯	⋯	⋯	Z_{JJ}^{rs}	⋯	⋯	⋯	⋯	⋯
		Industry S	Z_{J1}^{S1}	⋯	Z_{J1}^{SS}	⋯	Z_{JJ}^{S1}	⋯	Z_{JJ}^{SS}	F_{J1}^{S}	⋯	F_{JJ}^{S}	Y_{J}^{S}
Value Added			VA_{1}^{1}	⋯	VA_{1}^{S}	⋯	VA_{J}^{1}	⋯	VA_{J}^{S}				
Gross Output			Y_{1}^{1}	⋯	Y_{1}^{S}	⋯	Y_{J}^{1}	⋯	Y_{J}^{S}				

Appendix B Data Sources and Cleaning Procedures

We collect accounting and stock level data from COMPUSTAT Global and CRSP, following the data-cleaning and constructing procedures of Jensen et al. (2023). In order to match companies to OECD's TiVA industries, we use the reported NAICS industry code, which can be directly mapped to TiVA industries. For companies without a NAICS code, we use the following approach. We first construct a map between GICS and NAICS, using companies with both industry identifications available. We assign a GICS code to a NAICS code based on matching frequency. The NAICS with the largest number of matches to a given GICS is assigned as the NAICS code that corresponds to the given GICS code. Next, we convert all companies with an available GICS code to a NAICS code, which we then map to a TiVA industry. We collect information on stock returns, market equity, book equity, profitability (defined as operating profits scaled book equity), investment (defined as the annual growth rate of assets) and dividends (scaled by book equity). To account for short term reversal and momentum, we include lagged return and the cumulative return in the eleven months preceding the lagged return. Since we construct economy-industry level variables, we weight returns and characteristics using market value. To include an economy-industry portfolio in our asset pricing tests, we require at least 20 stocks. We collect data for the World Governance Indicators, the market capitalization of domestic companies, population, GDP per capita and inflation from the World Bank. From the OECD, we collect data on the fraction of the labour force with tertiary education and interest rates. For countries without interest rate data from OECD, we use IMF data. Interest rates for Argentina and Taiwan are from the countries respective central banks. The data on the number of deep-water ports is based on Lane and Pretes (2020). Exchange rates are from COMPUSTAT Global. We estimate economy-industry and economy betas using a CAPM model based on the past 60 months of data and the global market portfolio as a risk factor. We require at least 24 monthly observations to compute either beta. We further compute a transportation costs factor, following Barrot et al. (2019) and using their replication code and files. The beta with respect to transportation costs is similarly estimated using the past 60 months of data, requiring at least 24 valid economy-industry observations.

Appendix C Glossary of Network Terminology

C.1 Key TiVA Variables

$\boldsymbol{GX_j^s}$ Dollar value of gross exports of industry s in economy j

$\boldsymbol{VA_{i,j}^{r,s}}$ Dollar value added of the gross exports of industry s in economy j that stems from imported intermediate inputs from industry r in economy i

$\boldsymbol{FVA_{i,j}^{r,s}}$ Foreign value added by industry r in economy i to industry s in economy j, computed as $VA_{i,j}^{r,s}$ divided by GX_j^s. Note that any domestic links are set to zero, i.e. $FVA_{i,j}^{r,s} = 0$ if $i = j$.

C.2 Network Definitions and Variables

$\boldsymbol{G(V,E)}$ The directed graph representing trade in value-added among 77 economies and 45 industries, defined by the set of nodes $\boldsymbol{V}$ and the set of edges $\boldsymbol{E}$.

$\boldsymbol{V}$ The set of nodes (economy-industry pairs), comprising 3465 pairs (77 economies $\times$ 45 industries) denoted as $n(s,j)$ or v.

$\boldsymbol{E}$ The set of directed edges $e_{i,j}^{r,s}$ connecting two nodes $n(r,i)$ and $n(s,j)$, equal to the value added by industry r in economy i to industry s in economy j, i.e. $FVA_{i,j}^{r,s}$. Note that since $FVA_{i,j}^{r,s} = 0$ if $i = j$, all edges linking industries from the same economy are set to 0.

$\boldsymbol{P}$ A path in the graph $\boldsymbol{G}$ representing a collection of nodes $n(r,i)$ and directed edges $e_{i,j}^{r,s}$ that link them, forming a route from a source node to a target node.

$\boldsymbol{A}$ The adjacency matrix representing the connections between nodes in the network. The entry $A_{n(r,i),n(s,j)}$ in the matrix is $FVA_{i,j}^{r,s}$ if there exists a directed edge from $n(r,i)$ to node $n(s,j)$, and 0 otherwise.

$\boldsymbol{Length(P)}$ The length of a path is the number of nodes part of the path.

$\boldsymbol{DirectPath_{n(r,i)\to n(s,j)}}$ The direct path from node $n(r,i)$ to node $n(s,j)$ in the graph $\boldsymbol{G(V,E)}$, con-

sisting of the source node $n(r,i)$, the target node $n(s,j)$, and the edge connecting them $e_{i,j}^{r,s}$. It represents the direct value flows between the two nodes.

$\boldsymbol{ShortestPath_{n(r,i)\rightarrow n(s,j)}}$

The shortest path from node $n(r,i)$ to node $n(s,j)$ in the graph $\boldsymbol{G(V,E)}$, given by:

$$ShortestPath_{n(r,i)\rightarrow n(s,j)} = \arg\min_{P} \sum_{e\in P} c(e)$$

where P represents a path in $\boldsymbol{G}$, and $c(e)$ is the cost of an edge e along the path P equal to e^{-1}. This path minimizes the total accumulated *cost* between industry r in economy i and industry s in economy j. Because the costs are defined as the inverse of the edges, the shortest path represents the path with the strongest supply chain flows. See Opsahl et al. (2010) for an overview of the literature that uses weights as inverse of the edges and the application of the algorithm of Dijkstra (1959) for finding minimum cost paths in networks.

$\boldsymbol{Upstreamness_{n(s,j)}}$

Following Antràs et al. (2012) the upstreamness of a node is defined as the weighted average number of production stages the node is from final demand:

$$Upstreamness_{n(s,j)} = \boldsymbol{Y}^{-1} \cdot (1 \cdot \boldsymbol{I} + 2 \cdot \boldsymbol{A} + +3 \cdot \boldsymbol{A}^2 + \cdots) \cdot \boldsymbol{F}$$

C.3 Network Centrality Measures

Below the definition of the centrality measures used in this paper. We present a correlation matrix of the centrality measures in Table A1.

$\boldsymbol{CPV(v)}$ The Choke Point Value of node v is the betweenness centrality of node v, computed as the total number of shortest passing through the node, scaled by the total number of shortest paths in the network:

$$\sum_{n\neq v\neq t} \frac{\sigma_{n,t}(v)}{\sigma_{n,t}}$$

where $\sigma_{n,t}$ denotes the number of shortest paths from node n to node t and $\sigma_{n,t}(v)$ denotes the number of shortest paths from n to t that v lies on.

***EIGEN*(*v*)** The eigenvector centrality of node v, computed iteratively based on the connections of neighboring nodes and their own centralities:

$$\frac{1}{\lambda}\sum_{t\neq v} A_{v,t}\cdot EIGEN(t)$$

***KB*(*v*)** The Katz-Bonacich centrality of node v, computed based on the number of paths of varying lengths connecting v to other nodes, with a parameter α controlling the influence of distant nodes:

$$\alpha\sum_{t} A_{v,t} + \alpha^2\sum_{n\neq v} A_{v,n}\cdot A_{n,t} + \alpha^3\sum_{n\neq v} A_{v,n}\cdot A_{n,m}\cdot A_{m,t} + \ldots$$

***WIN*(*v*)** The weighted indegree centrality of node v, computed as the sum of the weights of incoming edges:

$$\sum_{n} A_{n,v}\cdot e_{n,v}$$

***CLO*^{IN}(*v*)** The in-closeness centrality of node v, computed as the reciprocal of the average shortest path cost (d) ending in v from all other nodes:

$$\frac{1}{\frac{1}{n-1}\sum_{n\neq v} d(n,v)}$$

***WOUT*(*v*)** The weighted outdegree centrality of node v, computed as the sum of the weights of outgoing edges:

$$\sum_{t} A_{v,t}\cdot e_{v,t}$$

***CLO*^{OUT}(*v*)** The out-closeness centrality of node v, computed as the reciprocal of the average shortest path cost (d) from v to all other nodes:

$$\frac{1}{\frac{1}{n-1}\sum_{t\neq v} d(v,t)}$$

***CENT*^{AVE}(*v*)**

Average centrality is the average of $CPV(v)$, $CLO^{OUT}(v)$ and $CLO^{IN}(v)$.

Table A1: Correlation of Network Centrality Measures in the Global Production Nework

This table presents a correlation matrix of network centrality measures. We compute Spearman correlations each year and then compute average values across all years.

	CPV	$EIGEN$	KB	WIN	CLO^{IN}	$WOUT$	CLO^{OUT}	$CENT^{AVE}$
Betweenness:								
CPV	1.00							
Foreign Dependence:								
$EIGEN$	0.41	1.00						
KB	0.41	1.00	1.00					
WIN	0.41	0.96	0.98	1.00				
CLO^{IN}	0.10	0.26	0.24	0.17	1.00			
Foreign Influence:								
$WOUT$	0.58	0.04	0.04	0.04	0.07	1.00		
CLO^{OUT}	0.62	0.11	0.11	0.09	0.18	0.92	1.00	
Average Centrality:								
$CENT^{AVE}$	0.35	0.19	0.18	0.11	0.84	0.46	0.58	1.00

Appendix D The Production Network and Choke Points in 2019

In this Appendix, we provide an overview of the distribution of choke points in 2019. Both Figure D.1 and Figure D.2 indicate the the topology of choke points was similar in 2019 to the one we present in the main body of the paper.

Figure D.1: Geographic Distribution of Choke Point Index in 2019

This figure depicts economy Choke Point Value (CPV) for 2019, computed as the number of shortest paths passing via a economy, expressed as a percentage of all shortest paths. Higher intensity of blue represents higher economy CPV. Countries with no data are depicted in light gray.

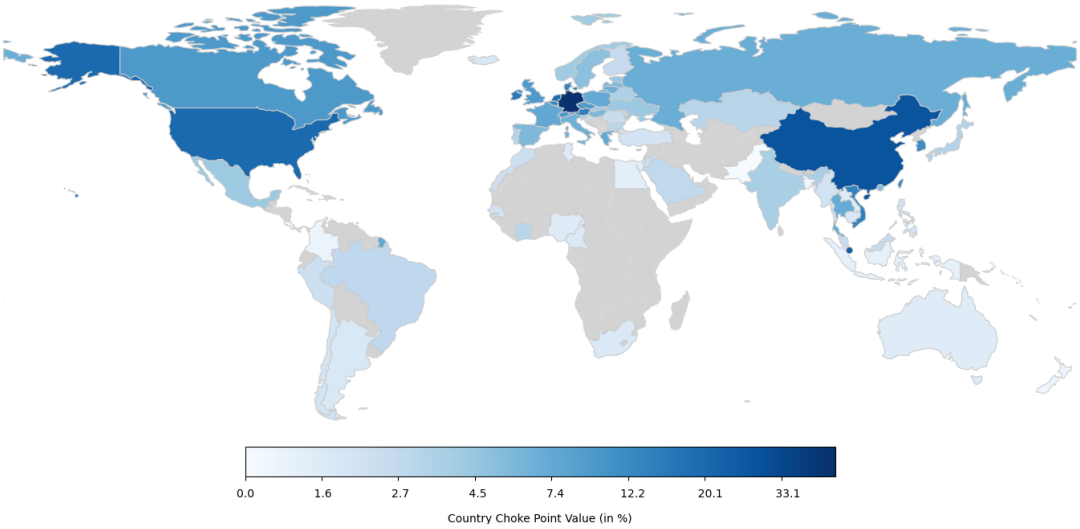


Figure D.2: The Global Network of Choke Points in 2019

This figure presents a visual representation of the global network of choke points in 2019, where each node is an economy-industry pair. The thickness of the arrow from node A to node B represents the total number of shortest paths passing from node A to node B. The size of the node represents the total number of shortest paths passing via the node, i.e. the node's Choke Points Value. We group nodes into seven groups, based on the geography and economic development, following the classification in Table 1. Within each group of nodes, we place all manufacturing industries in the outer circle, all business services industries in the middle cirlce, and all other industries in the inner circle.

